

<https://helda.helsinki.fi>

Spatial and temporal patterns of Holocene precipitation change in the Iberian Peninsula

Ilvonen, Liisa

2022-10

Ilvonen , L , Lopez-Saez , J A , Holmstrom , L , Alba-Sanchez , F , Perez-Diaz , S , Carrion , J S , Ramos-Roman , M J , Camuera , J , Jimenez-Moreno , G , Ruha , L & Seppä , H 2022 , ' Spatial and temporal patterns of Holocene precipitation change in the Iberian Peninsula ' , *Boreas* , vol. 51 , no. 4 , pp. 776-792 . <https://doi.org/10.1111/bor.12586>

<http://hdl.handle.net/10138/349994>

<https://doi.org/10.1111/bor.12586>

cc_by

publishedVersion


Downloaded from Helda, University of Helsinki institutional repository.

This is an electronic reprint of the original article.

This reprint may differ from the original in pagination and typographic detail.

Please cite the original version.

Spatial and temporal patterns of Holocene precipitation change in the Iberian Peninsula

LIISA ILVONEN , JOSÉ ANTONIO LÓPEZ-SÁEZ, LASSE HOLMSTRÖM, FRANCISCA ALBA-SÁNCHEZ, SEBASTIÁN PÉREZ-DÍAZ, JOSÉ S. CARRIÓN, MARÍA J. RAMOS-ROMÁN, JON CAMUERA, GONZALO JIMÉNEZ-MORENO, LEENA RUHA AND HEIKKI SEPPÄ

BOREAS



Ilvonen, L., López-Sáez, J. A., Holmström, L., Alba-Sánchez, F., Pérez-Díaz, S., Carrión, J. S., Ramos-Román, M. J., Camuera, J., Jiménez-Moreno, G., Ruha, L. & Seppä, H. 2022 (October): Spatial and temporal patterns of Holocene precipitation change in the Iberian Peninsula. *Boreas*, Vol. 51, pp. 776–792. <https://doi.org/10.1111/bor.12586>. ISSN 0300-9483.

Precipitation is a key climate parameter of vegetation and ecosystems in the Iberian Peninsula. Here, we use a regional pollen–climate calibration model and fossil pollen data from eight sites from the Atlantic coast to southern Spain to provide quantitative reconstructions of annual precipitation trends and excursions and their regional patterns for the last 11 700 years. The Early Holocene (11 700 to 11 000 cal. a BP) was characterized by high precipitation values followed by a slowly declining trend until about 9000 cal. a BP in the south and about 8000 cal. a BP in the north. From 8000 to 6000 cal. a BP the reconstructed precipitation values are the highest in most records, especially in those located in the Mediterranean climatic region in the southern part of the peninsula, with maximum values nearly 100% higher than the modern reconstructed values. The results suggest a declining precipitation during the Late Holocene in the south, with a positive excursion at around 2500 cal. a BP, while in the north precipitation remained high until 500 cal. a BP. However, the Late Holocene climate reconstructions in the Iberian Peninsula are biased by intensifying human impact on vegetation. The statistical time series analyses using SiZer technique do not indicate any statistically significant high-frequency drought events in the region. In general, our results suggest regional differences in the precipitation patterns between the northern and southern parts of the peninsula, with a more distinct Middle Holocene period of high humidity in the south.

Liisa Ilvonen (liisa.ilvonen@helsinki.fi), Department of Geosciences and Geography, University of Helsinki, P.O. Box 64, FI-00014 Helsinki, Finland and Organismal and Evolutionary Biology Research Programme, Research Centre for Ecological Change, University of Helsinki, P.O. Box 65, FI-00014 Helsinki, Finland; José Antonio López-Sáez, Instituto de Historia, CSIC, c/ Albasanz 26–28, 28037 Madrid, Spain; Lasse Holmström, Research Unit of Mathematical Sciences, University of Oulu, P.O. Box 8000, FI-90014 Oulu, Finland; Francisca Alba-Sánchez, Department of Botany, University of Granada, 18071 Granada, Spain; Sebastián Pérez-Díaz, Department of Geography, Urban and Regional Planning, University of Cantabria, Avda. de los Castros s/n, 39005 Santander, Spain; José S. Carrión, Department of Plant Biology, Faculty of Biology, University of Murcia, 30100 Espinardo, Murcia, Spain; María J. Ramos-Román, Jon Camuera and Heikki Seppä, Department of Geosciences and Geography, University of Helsinki, P.O. Box 64, FI-00014 Helsinki, Finland; Gonzalo Jiménez-Moreno, Department of Stratigraphy and Palaeontology, University of Granada, 18071 Granada, Spain; Leena Ruha, Natural Resources Institute Finland, Paavo Havaksen tie 3, 90570 Oulu, Finland; received 14th September 2021, accepted 14th January 2022.

Successful use of quantitative transfer functions for climate reconstructions from pollen and other biological proxy data has many requirements. Of particular importance is that the reconstructions must be focused on regions where the palaeorecords are climatologically sensitive to the climate variable of interest and where it is possible to construct high-quality modern calibration sets (Birks 1995). Within the scope of pollen-based climate reconstructions, such regions are where there exists a simple zonal climatic gradient, determined or strongly influenced by one or a few dominant climatic variables, and where there exists equally clear vegetation zonation determined by these dominant climatic variables (Seppä *et al.* 2004). The Iberian Peninsula is one such region, as it is a climatic transition area between the Atlantic and the Mediterranean and subtropical to middle-latitude climate gradients (Lionello *et al.* 2006). It displays wide regional climate variability and large gradients, especially following a north–south transect (Karagiannidis *et al.* 2008), constituting thus a small-

scale coupled sea–atmosphere system with a short time response to climatic forcing (Xoplaki *et al.* 2004). The Mediterranean climate is also influenced by weather conditions over the Atlantic and sometimes by polar outbreaks. One key factor of the Mediterranean climate is its seasonality, marked by a strong annual precipitation cycle between dry summers and wet winters (Dünkeloh & Jacobeit 2003; Lionello *et al.* 2006).

Since the majority of the Mediterranean ecosystems are water limited and depend on the seasonal and temporal dynamics of precipitation (Blondel *et al.* 2010), the Mediterranean forests are highly vulnerable to past and future climate changes. It is expected that by 2100 the annual rainfall will have dropped by up to 20% (up to 50% less in summer), and the mean temperatures will have increased by 3–4 °C (Solomon *et al.* 2007; Giorgi & Lionello 2008). During recent decades, the intensity and frequency of drought and fire events have increased in the Mediterranean region (Solomon *et al.* 2007). Even more extreme droughts and warmings have been reported in the

palaeoclimatological data (Carrión *et al.* 2010; Tarroso *et al.* 2016). Precipitation has been a key climatic variable both in the history of vegetation and in the demographic and cultural dynamics of the Mediterranean Basin, and particularly in the Iberian Peninsula (Ninyerola *et al.* 2007; Benito-Garzón *et al.* 2008; Pontevedra-Pombal *et al.* 2017), where a combination of archaeological and palaeoenvironmental studies show the influence of abrupt climatic events on settlement patterns and selective methods of anthropogenic exploitation of ecosystems (Carrión *et al.* 2010; Lillios *et al.* 2016; Blanco-González *et al.* 2018; Alba-Sánchez *et al.* 2021).

Given the steep gradients and the coupling between vegetation and water availability, past vegetation changes in the Iberian Peninsula provide a means to investigate past water availability and precipitation changes. In recent decades, a number of studies based on lake level, pollen and speleothem data have dealt with climate reconstructions in the Iberian Peninsula and adjacent seas (Peñalba *et al.* 1997; Combourieu Nebout *et al.* 2009; Dormoy *et al.* 2009; Morellón *et al.* 2009, 2018; Fletcher *et al.* 2010; Jiménez-Moreno *et al.* 2015; Tarroso *et al.* 2016; Ramos-Román *et al.* 2018a, b; Schröder *et al.* 2018). Many of these reconstructions have indicated consistent Holocene trends, with more humid Middle Holocene conditions followed by increasing aridity in the last 5000 years (Morellón *et al.* 2009; Ramos-Román *et al.* 2018b; Schröder *et al.* 2018). However, the timings of the main climatic periods, such as the more humid Middle Holocene, vary in different records. It is possible that these inconsistencies between reconstructions reflect partly different techniques used in investigations and partly regional climate anomalies in the Iberian Peninsula.

To investigate the Holocene humidity trends and events in different parts of the Iberian Peninsula, we report here pollen-based quantitative precipitation reconstruction results based on a transfer function approach from eight pollen records following a north–south transect from the Atlantic to the Mediterranean climatic domains. We use two different reconstruction techniques, one based on weighted average partial least squares (WAPLS) and another based on Bayesian modelling. To provide a regional synthesis of the precipitation and humidity changes, we compare our pollen-based precipitation reconstructions with independent records of humidity, such as the lake-level data from the Iberian Peninsula and the North-Atlantic Oscillation (NAO) reconstruction. To statistically test whether the wiggles in the reconstruction curves are statistically significant, we apply a new version of the SiZer (“SIgnificant ZERo crossings of derivatives”) analysis. As statistical detection of short-lived anomalies normally requires high-resolution data, we combine our individual records to two stacks (northern Iberian Peninsula and southern Iberian Peninsula) to detect whether our datasets demonstrate any regional anomalies in the Holocene precipitation patterns.

Study area

Our study area is in the Iberian Peninsula following a north–south transect from latitude 43°47'N to 36°01'N and from longitude 9°30'W to 3°19'E, encompassing several mountain ranges. The mean elevation of the Iberian Peninsula is around 660 m a. s. l. The climate of the peninsula is divided into two major climate zones: (i) the Atlantic climate characterized by mild summers and cold, rainy winters; and (ii) the Mediterranean climate with mild winters and hot, dry summers (Capel 2000). The Atlantic Ocean influences the northern and western parts of the peninsula, and the Mediterranean Sea influences the south (Fig. 1). The coastline is under the influence of the Atlantic Ocean in the north and the west, and the Mediterranean Sea in the south and the east. The lowest temperatures are measured in the regions influenced by the Atlantic Ocean and the highest in the regions adjacent to the Mediterranean Sea. In addition to the general north–south climatic gradient, seasonal and diurnal thermal gradients stretch from the coast to the centre of the peninsula (Dasari *et al.* 2014). From a biogeographical point of view, the Atlantic bioregion extends from Galicia to northern Portugal, Asturias, Cantabria, the Basque Country and the western and central Pyrenees. It is characterized by a wet climate, moderated by the oceanic influence, with temperate-cold winters and no clearly defined dry season. The Mediterranean bioregion incorporates all inland plateaus and mountains as well as the Mediterranean basin zones (Rivas-Martínez 2007). The main vegetation types vary from semi-desertic flora, Mediterranean oak forests, steppeland areas and evergreen pine forests to deciduous and high-mountain pine forests, and subalpine and alpine vegetation (Blanco-Castro *et al.* 1997; Loidi, 2017).

Material and methods

Data sources

The use of transfer functions for quantitative climate reconstructions requires a collection of modern pollen samples that can be used as a calibration model in the reconstruction. Our modern pollen–climate calibration model includes 236 modern pollen samples with known modern annual precipitation (P_{ann}) values, analysed for the relative abundances of 136 pollen taxa (Fig. 1). Modern pollen surface samples (moss pollsters) were collected with positional and altitudinal data recorded using a portable GPS device, following north–south and east–west transects in Spain (Fig. 1). Several moss samples were randomly collected on the ground at each site within an area of 100 m² and homogenized into one sample. The collection approach ensured a representative sampling of flora with either long- or short-range pollen dispersal and also minimized local overrepresent-

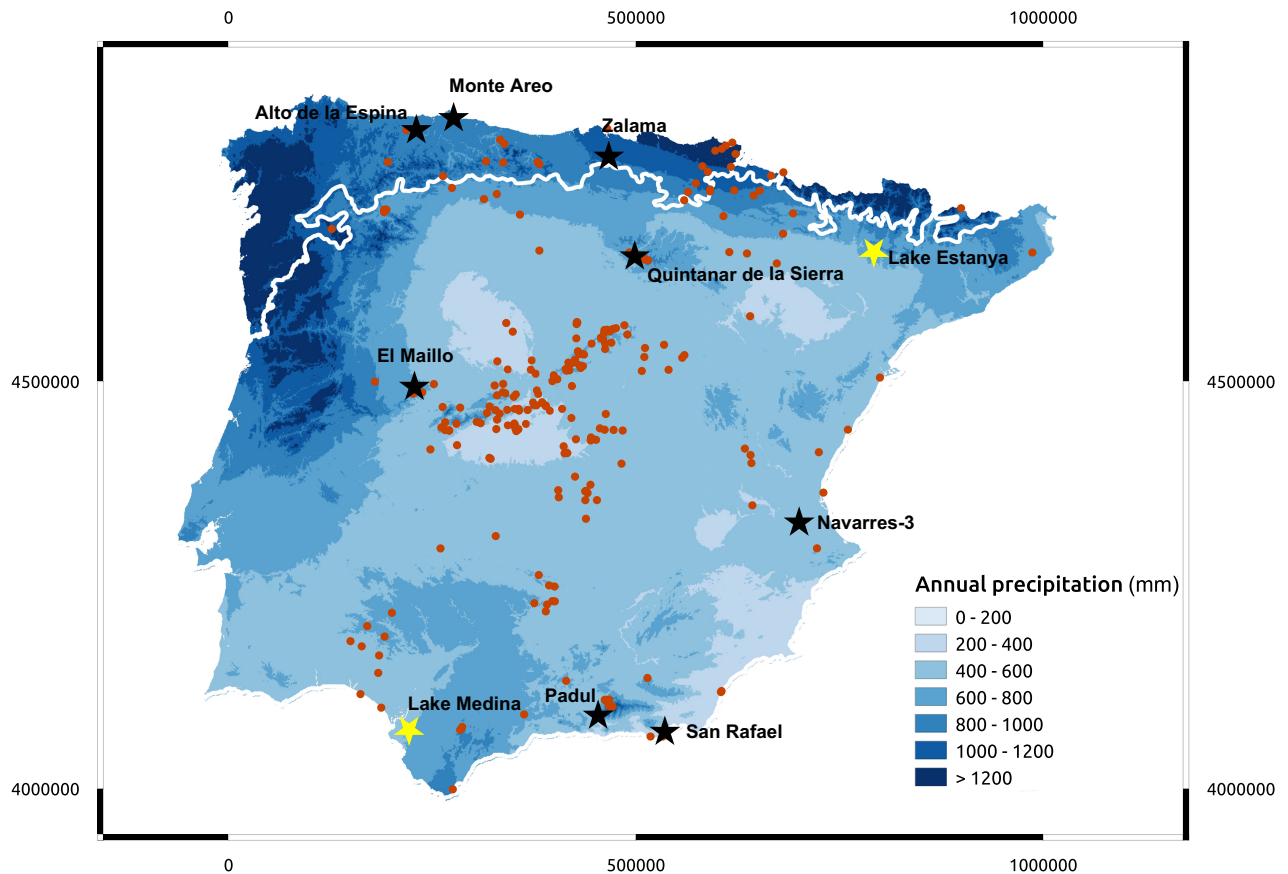


Fig. 1. Locations of modern pollen samples, cores and lakes with lake-level reconstructions. Modern pollen samples are denoted by red dots and cores are denoted by black stars. The yellow stars denote the lake record locations from Lake Medina and Lake Estanya (see Fig. 5). The colours in the map indicate the modern P_{ann} (annual precipitation) values. The white line indicates the boundary between the Atlantic (Eurosiberian) and Mediterranean biogeographical regions. Table S1 shows longitude, latitude, P_{ann} , altitude and local vegetation type for each modern pollen sample site.

tation of single species. Sites were chosen using the vegetation map of Spain (Rivas-Martínez 2007) to properly characterize the major vegetation communities. The samples were treated with standard techniques (Moore *et al.* 1991). All of the pollen samples in the calibration model were treated in the laboratory and analysed under the microscope by one person (José Antonio López-Sáez) to ensure the taxonomical harmonization of the 236 selected pollen samples. The identification of critical pollen morphotypes, for example those in the *Pinus* and *Quercus* genera, was carried out in a consistent manner as described in Carrión *et al.* (2000b) and López-Sáez *et al.* (2010, 2015, 2020).

A minimum of 500 pollen of taxa belonging to the sum of terrestrial pollen were counted. All terrestrial pollen types were used in the climate reconstructions while aquatic taxa and spores were excluded from the pollen sum. To establish criteria of standardization and consistency in the data and to reduce bias, only taxa with percentages >1% and present in at least 5% of the samples were included. Following this procedure, 136 pollen taxa were selected, and the percentages were recalculated

accordingly. Modern annual precipitation values were obtained from the WorldClim database (Fick & Hijmans 2017) with a 30 s resolution (approximately 1 km²). Annual precipitation values for the surface sites range from 231 to 1327 mm. For more details on the modern pollen samples see López-Sáez *et al.* (2010, 2013, 2015) and Davis *et al.* (2013, 2020). Some modern pollen samples are available at the European Pollen Database, included in Neotoma Database (www.neotomadb.org) and they can be identified based on comparing their coordinates in our Table S1 and in the aforementioned database. Additional information about sites is available in Table S1. In addition, modern pollen samples can be viewed online using a map-based viewer at <https://empd2.github.io>.

The records on which the past precipitation reconstructions are based comprise eight pollen records from bogs and wetlands: Alto de la Espina (or La Molina), El Maillo, Monte Areo, Navarres-3, Quintanar de la Sierra, Padul-15-05, San Rafael and Zalama (Fig. 1). These records were selected as they represent different climatic regions of the Iberian Peninsula from the more humid

Table 1. Information on the eight fossil pollen records.

Site	Latitude N	Longitude W	Elevation (m a.s.l.)	P_{ann} (mm)	References
Alto de la Espina	43°22'52"	6°19'38"	650	930	López-Merino <i>et al.</i> (2011, 2014)
El Maíllo	40°32'48"	6°12'35"	1100	715	Morales-Molino <i>et al.</i> (2013)
Monte Areo	43°31'44"	5°46'08"	200	881	López-Merino <i>et al.</i> (2010)
Navarrés-3	39°05'36"	0°41'00"	225	429	Carrión & van Geel (1999)
Padul-15-05	37°00'40"	3°36'14"	725	445	Ramos-Román <i>et al.</i> (2018a, b)
Quintanar de la Sierra	42°01'31"	3°01'34"	1470	743	Peñalba (1994)
San Rafael	36°46'25"	2°36'05"	0	231	Pantaléon-Cano <i>et al.</i> (2003)
Zalama	43°08'06"	3°24'35"	1330	1059	Pérez-Díaz <i>et al.</i> (2016)

northwestern parts to the dry regions in the south. They were gathered from the European Pollen Database (<http://www.europeanpollendatabase.net>) or the Spanish research project Paleodiversitas (Carrión 2015), or directly provided by researchers (Table 1). The pollen data from Quintanar de la Sierra have been used earlier for quantitative climate reconstructions by Peñalba *et al.* (1997). Pollen percentages (Fig. S1) were calculated from terrestrial pollen sums, excluding aquatic plants. The sites Alto de la Espina, Monte Areo and Zalama are located in the Atlantic region, while El Maíllo, Navarrés-3, Padul-15-05, Quintanar de la Sierra and San Rafael are located in the Mediterranean region (Fig. 1). In the Atlantic region, Zalama is located at the highest altitude, followed by Alto de la Espina and Monte Areo. Quintanar de la Sierra belongs biogeographically to the Mediterranean region, but is located in the heart of the Northern Iberian Range that can be considered as an island of Atlantic vegetation. El Maíllo is located in the valley area of the peninsular centre and Navarrés-3 is in an area close to the coast of the Mediterranean Sea. Padul-15-05 and San Rafael are in the most southeastern zone.

The chronologies of all sites are based on radiocarbon dating. In order to produce a chronology for each fossil pollen record we used a Bayesian age–depth model called Bchron (Haslett & Parnell 2008). Bchron first calibrates radiocarbon dates with a calibration curve and then fits the age–depth model, which is consistent with the calibrated radiocarbon dates. Assumptions for the age–depth model are continuous, monotone and piecewise linear age–depth dependence. The age for the uppermost sediment of the core was assumed to be the year when the core was extracted. Fig. 2 shows the results of the eight Bchron runs (see Table S4 for radiocarbon date data). The figure shows the posterior distributions of the calibrated radiocarbon dates, the posterior mean chronology and the 95% credible intervals for the possible chronologies. For Alto de la Espina, Monte Areo, El Maíllo, Zalama, Padul-15-05 and Quintanar de la Sierra the Bchron chronologies seem to be reliable for the whole core. For San Rafael five AMS dates suggest a fairly stable and reliable Holocene sedimentation rate. The Navarrés-3 core, however, ends

about 3000 cal. a BP, thus missing the Late Holocene part, making this sequence a chronologically floating sequence (Fig. 2). All ages in the text are expressed as cal. a BP.

Reconstruction of past climate variables

The selection of the climate variable of interest is a critical step in quantitative climate reconstructions (Li *et al.* 2015). In the Iberian Peninsula, and in larger context in the whole Mediterranean region, where summers are hot and dry, water availability is generally considered the critically important climatic variable for plant populations and communities, and its regional and temporal changes greatly influence the vegetation structure and composition (Vicente-Serrano *et al.* 2014; Samartin *et al.* 2017; Vidal-Macua *et al.* 2017). However, the summer temperature may also be an important factor, especially at more mesic sites and at the high altitudes (Pasho *et al.* 2011; Vidal-Macua *et al.* 2017). It is realistic to accept that no single climatic variable can account for the complete influence of climate on vegetation and that no single or a few reconstructed climate variables can capture the full spectrum climate patterns and changes in the past. The eight pollen records were selected from altitudes lower than 1500 m a.s.l., and the climate variable that we have reconstructed is P_{ann} . In our study region, P_{ann} is an ecologically important and conceptually simple variable, which can be used in comparison with other palaeoclimate records and model simulations. Precipitation has a clear zonal pattern in the Iberian Peninsula, and its importance for vegetation patterns is reflected by the comparable zonation of vegetation. In the leave-one-out cross-validation test, P_{ann} has a high R^2 and a low RMSEP (Table 2), demonstrating that it accounts for a large proportion of variance in the precipitation-related climatic patterns in the region.

We use two different, complementary quantitative techniques, WAPLS and Bayesian modelling to produce the past precipitation reconstructions from the eight pollen records. With both techniques, all 236 modern pollen samples were used to calculate the transfer functions for modern annual precipitation. In all cases,

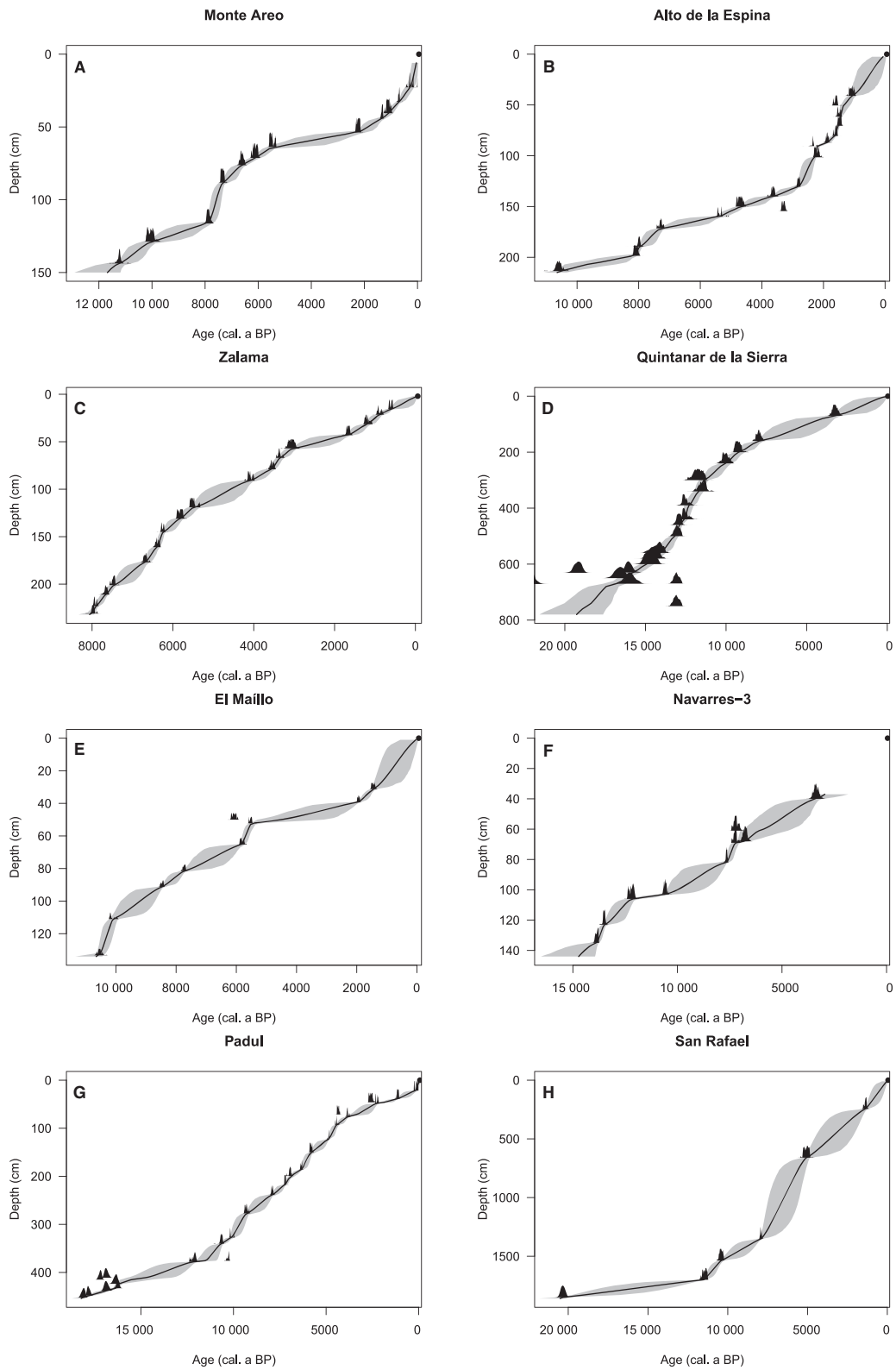


Fig. 2. Outputs of Bchron chronology model run for the eight cores used in precipitation reconstructions for Monte Areo (A), Alto de la Espina (B), Zalama (C), Quintanar de la Sierra (D), El Maíllo (E), Navarres-3 (F), Padul-15-05 (G) and San Rafael (H). The posterior distributions of the calibrated radiocarbon dates are shown in black; the grey lines indicate the radiocarbon dated depths and the 95% credible intervals for the reconstructions we use posterior mean chronologies. The solid black line is the posterior mean chronology and the dot marks the top of the core. In the reconstructions we use posterior mean chronologies.

Table 2. Information and performance statistics of the modern pollen–climate calibration model. Reported statistics based on leave-one-out cross-validation are root mean square error of prediction (RMSEP), coefficient of determination (R^2) and maximum bias. The WAPLS statistics are based on a two-component model.

Number of sites	236
Precipitation gradient	231–1327 mm
Precipitation range	1096 mm
Number of taxa	136
WAPLS RMSEP	144.71 mm
WAPLS R^2	0.61
WAPLS maximum bias	328.08 mm
Bayesian model RMSEP	170.82 mm
Bayesian model R^2	0.55
Bayesian model maximum bias	239.53 mm

we used a two-component WAPLS model by ter Braak & Juggins (1993). Calibration model pollen data values (as percentages) were square root transformed for WAPLS regression to reduce noise in the data. Calculation of WAPLS transfer functions was performed in the C2 programme (Juggins 2007). The Bayesian reconstruction method used is based on Bummer, a Bayesian hierarchical multinomial regression model introduced in Vasko *et al.* (2000). In the basic Bummer model, the observed pollen taxon relative abundances are modelled by a multinomial distribution, where the taxon occurrence probabilities are treated as Dirichlet-distributed random variables whose distribution is determined by the environmental response parameters of the pollen taxa, as well as the mean annual precipitation. The taxon environmental response is modelled by a unimodal Gaussian function, with shape and mean determined by the response parameters α (scale), β (optimal precipitation) and γ (tolerance) (see Fig. S2). The prior distributions of the model parameters are listed in Table S2.

The major difference between the WAPLS and Bayesian modelling is that WAPLS assumes that parameters to be estimated are fixed and the data are random observations from some population. However, in Bayesian modelling parameters are treated as random variables and the data are fixed. In Bayesian modelling, we learn from the parameters by combining the observed data and the prior distribution, which formulates our prior knowledge about the model parameters. In the prior distribution, it is possible to bring useful climatic knowledge to the model, which is not possible in the WAPLS method. While WAPLS is often used for quantitative reconstructions (Juggins & Birks 2012; Chevalier *et al.* 2020), the Bayesian modelling provides some potential advantages, such as joint inferences about the parameters of interest and clearer modelling of uncertainty, in climate reconstructions (Parnell *et al.* 2016).

The performance of both transfer functions was evaluated by leave-one-out cross-validation (Birks *et al.* 1990). Based on the leave-one-out cross-validation results we calculated the coefficient of determination

(R^2), root-mean-square error of prediction (RMSEP) and maximum bias as performance statistics.

Regional stacks

To compare the precipitation trends between northern Iberian Peninsula and southern Iberian Peninsula we constructed synthesis records for both regions by combining individual records to stacks. The northern stack includes data from Alto de la Espina, Monte Areo and Zalama and the southern stack from Padul-15-05, San Rafael and Navarrés-3. Quintanar de la Sierra and El Maillo were excluded from these stacks as they are located in central Spain. The stacks were made only with the WAPLS-based reconstructions, by first calculating the deviation from the mean P_{ann} of the individual records and then combining the deviations from the mean in chronological order for stacks. The advantage of such stacks is that compared with individual records they include a higher number of samples and thus higher temporal resolution, making it more feasible to detect short-term events in the dataset, especially when using statistical tools.

Detection of significant features in the regional stacks

Stacks were further analysed using the SiZer method. SiZer is an inference tool, which is designed to statistically detect significant features in time series data in various smoothers fitted to the original data (Chaudhuri & Marron 1999). SiZer has shown its usefulness, for example, in palaeoclimatology and ecology (Korhola *et al.* 2000; Eröstö & Holmström 2006; Weckström *et al.* 2006; Olsen *et al.* 2008; Divine *et al.* 2009; Clements & Rohr 2009; Sonderegger *et al.* 2009; Clements *et al.* 2010; Eröstö *et al.* 2012; Godliebsen *et al.* 2012; Miettinen *et al.* 2012). The strength of SiZer is that it makes few model assumptions and is therefore suitable for a broad range of climatological time series analysis. SiZer applies a non-parametric smoother to the palaeoclimatic data, and then examines the derivatives of the smoothed curve to identify the existence of statistically significant anomalies at different frequency levels (Chaudhuri & Marron 1999). When used for time series, SiZer analysis applies a non-parametric smoothing to a signal and detects the time intervals with a significantly increasing or decreasing smoother. A wide range of smoothing levels is used to reveal the salient features in the signal at all frequency levels.

In the traditional SiZer analysis, the results are visualized using a colour graph where the time is on the horizontal axis and the smoothing level is on the vertical axis, and for each pixel, its colour represents the significance of the derivative of the smoother for the corresponding time point and scale. Such a graph is an efficient tool to discover all of the significant declines and rises in the data at a glance. However, as the graph only shows the significance of the derivatives, it does

not allow comparison of the magnitudes of the derivatives within or between scales. While the within-scale comparison could be achieved by tinting the colours of pixels with respect to the derivatives of the smoother, this does not allow comparison between scales as the magnitude of derivatives of a smoother declines with increased smoothing. For this reason, we enhanced the informativeness of the graphs by tinting the colour of the significantly positive or negative derivatives with respect to the magnitude of the so-called normalized derivative (Lindeberg 1998), enhancing the comparison of declines and rises between and within scales. Thus, higher intensities of the tint (darker colours) suggest stronger declines (or rises) than the lighter intensities of tint (lighter colours). The colour-enhanced SiZer analyses were performed by modifying accordingly the source code of the SiZer package (Sonderregger 2012) in R 3.1.2 (R Development Core Team 2020).

Results

Transfer function performance

Leave-one-out cross-validation performance statistics (R^2 , RMSEP and maximum bias) for the two-component WAPLS and Bayesian transfer functions are shown in Fig. 3 and Table 2. The R^2 between the observed modern precipitation values and those predicted by WAPLS (based on the leave-one-out cross-validation) is 0.61. The R^2 for the Bayesian model is 0.55 respectively. Furthermore, the RMSEP is 145 mm with WAPLS and 170 mm with the Bayesian model. Thus, the WAPLS slightly outperforms the Bayesian model as measured with RMSEP, R^2 and maximum bias. One potential reason for this is that we used a wide prior in the Bayesian model for the predicted precipitation to not restrict the precipitation values too much a priori. Fig. 3 shows that both models underestimate the precipitation values at the high end of the precipitation gradient. For lower precipitation values along the precipitation gradient we do not observe any systematic bias for either model. When these performance statistics are compared with other validation tests with WAPLS and Bayesian-based transfer functions, it can be seen that they are reasonably high, but still slightly lower than in other regional models. For example, in northern Europe, R^2 values between the predicted and observed summer or annual mean temperature values are generally 0.7–0.85 (Seppä & Bennett 2003; Birks & Seppä 2004), in China for P_{ann} the R^2 is 0.8 (Li et al. 2016) and in training sets from the Swiss Alps it is as high as 0.9 for mean summer temperature (Lotter et al. 2000).

Holocene trends

The P_{ann} values in the earliest Holocene (>10 000 cal. a BP) are high in most records, especially those based on the WAPLS technique. For example, the Quintanar de la

Sierra record is characterized by a marked peak in the P_{ann} values, up to over 1000 mm at 11 600 cal. a BP, followed by a progressive decline to under 800 mm until 8200 cal. a BP (Fig. 4). Monte Aro, Navarrés-3 and San Rafael show similar features with a period of maximum P_{ann} values at ~11 600 to 11 000 cal. a BP and a later period with progressively decreasing values until 9000 to 8000 cal. a BP (Fig. 4). The stack curve for northern Iberia shows a clear decreasing trend from the highest precipitation values at the beginning of the Holocene to around 8000 cal. a BP. A similar decreasing trend can be seen in the stack curve from southern Iberia, turning to a gradual increase after 9000 cal. a BP (Fig. 5).

The Middle Holocene from 8000 to 4200 cal. a BP is characterized by higher P_{ann} values in most of the reconstructions. Again, the trend is clearer in the WAPLS-based reconstructions (Fig. 4). The P_{ann} values exceed 1000 mm in Alto de la Espina and Monte Aro in the Atlantic region and 900 mm in Quintanar de la Sierra. San Rafael, Padul-15-05 and Navarrés-3, the three records located in the Mediterranean region, have their highest P_{ann} values in the Middle Holocene, with mean values between 400 and 600 mm. The Zalama and El Maíllo records are clear exceptions from this general trend, as in these records the P_{ann} values remain constant around 900 mm. However, in most cases, the reconstructed P_{ann} values are above the Holocene means and the Middle Holocene is thus the longest and most prominent humid period reflected in our records.

Our records suggest a declining general trend of P_{ann} over the last 4000 years in the Mediterranean climatic region (Figs 4, S3, Table S3). This is clearest in the records from Quintanar de la Sierra, Padul-15-05 and San Rafael, where the P_{ann} values decline to about 500–200 mm from the Middle Holocene P_{ann} maximum. The stack record suggests that this general P_{ann} decline was interrupted by a period of higher values of 2500 to 1800 cal. a BP (Fig. 5). In the records from the Atlantic region, no similar Late Holocene decrease can be observed. The Zalama and the Monte Aro records show a fairly stable P_{ann} trend up to present, except for the sudden drop in Monte Aro over the last few centuries. In the Alto de la Espina record, a short-lived peak of anomalously high P_{ann} values is indicated at 1500 cal. a BP. As shown in the pollen diagram, these values are caused by the exceptionally high *Pteridium* spore values, reaching a maximum of up to 83% at 1500 cal. a BP (Fig. S1). Such a peak of *Pteridium* is clearly an anomaly, probably caused by a local overrepresentation of *Pteridium* population at the coring site on the Alto de la Espina bog.

SiZer results

Based on the SiZer results, the most notable event in the northern stack is the rapid increase in P_{ann} at 8000 cal. a BP (Fig. 6). At a lower frequency level, the decline during the last 1500 cal. a BP is indicated as a statistically

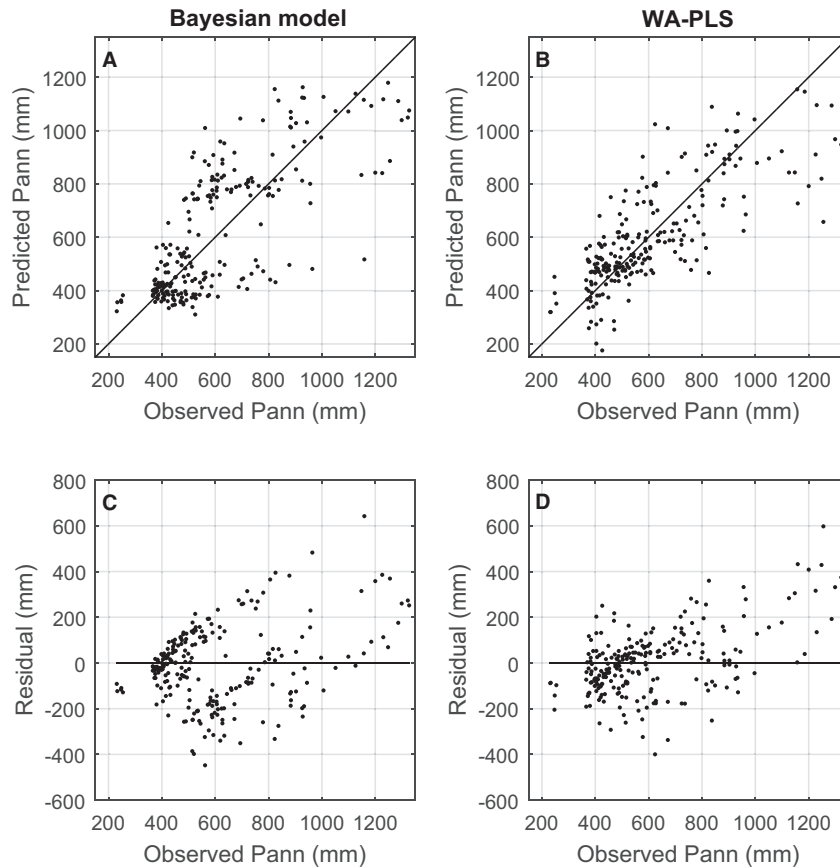


Fig. 3. Plots of predicted vs. observed modern P_{ann} (A and B) and the residual plots (C and D) for the Bayesian model and the two-component WAPLS in leave-one-out cross-validation. In the residual plot the differences between observed and predicted P_{ann} values (residuals) are plotted against observed P_{ann} values.

significant feature. In the southern stack, the most distinct statistically significant high-frequency event is the increase during the last 200 years. This apparent feature is caused by the anomalously high P_{ann} value in the top (modern) pollen sample of the Padul-15-05 and San Rafael cores (Fig. 4). The second clearest event in the southern stack is the negative anomaly at roughly 1500 cal. a BP. As discussed earlier, this sudden decline in the P_{ann} values may be partly an artefact caused by human impact on vegetation and it is thus not realistic to argue for any special climatic event at that time in the southern region. As in the north, there is also a low-magnitude positive P_{ann} event at 8000 cal. a BP in the southern stack. Thus, the shift toward higher P_{ann} at 8000 cal. a BP is the only statistically significant feature which can be seen both in the southern and northern stacks of the Iberian Peninsula.

Discussion

Model performance

A number of reasons can explain the slightly lower performance statistics of the pollen–climate calibration

model in the Iberian Peninsula as compared with northern Europe. One undeniable factor is the long-lasting and intense human impact that causes bias in climate–vegetation relationships (Carrión *et al.* 2000a; López-Sáez *et al.* 2016) and blurs the performance of the pollen–climate transfer functions (Li *et al.* 2015). Another likely factor is that the fossil pollen samples and modern samples in the calibration model represent different sedimentary environments. Besides having consistent taxonomy and nomenclature and being of comparable quality, the modern pollen data should be from the same sedimentary environment and basins of comparable size as the fossil datasets used for reconstruction purposes (Seppä *et al.* 2004; Birks *et al.* 2010). In this case the fossil assemblages are from mires and lakes, but the modern samples in the calibration model represent locally integrated moss samples. Lakes are scarce in many parts of the Iberian Peninsula and it is not possible to use samples from lakes only to construct a representative calibration model but we need to use samples from other sedimentary environments as well. This is a common problem when constructing pollen–climate transfer functions in dry and semidry regions,

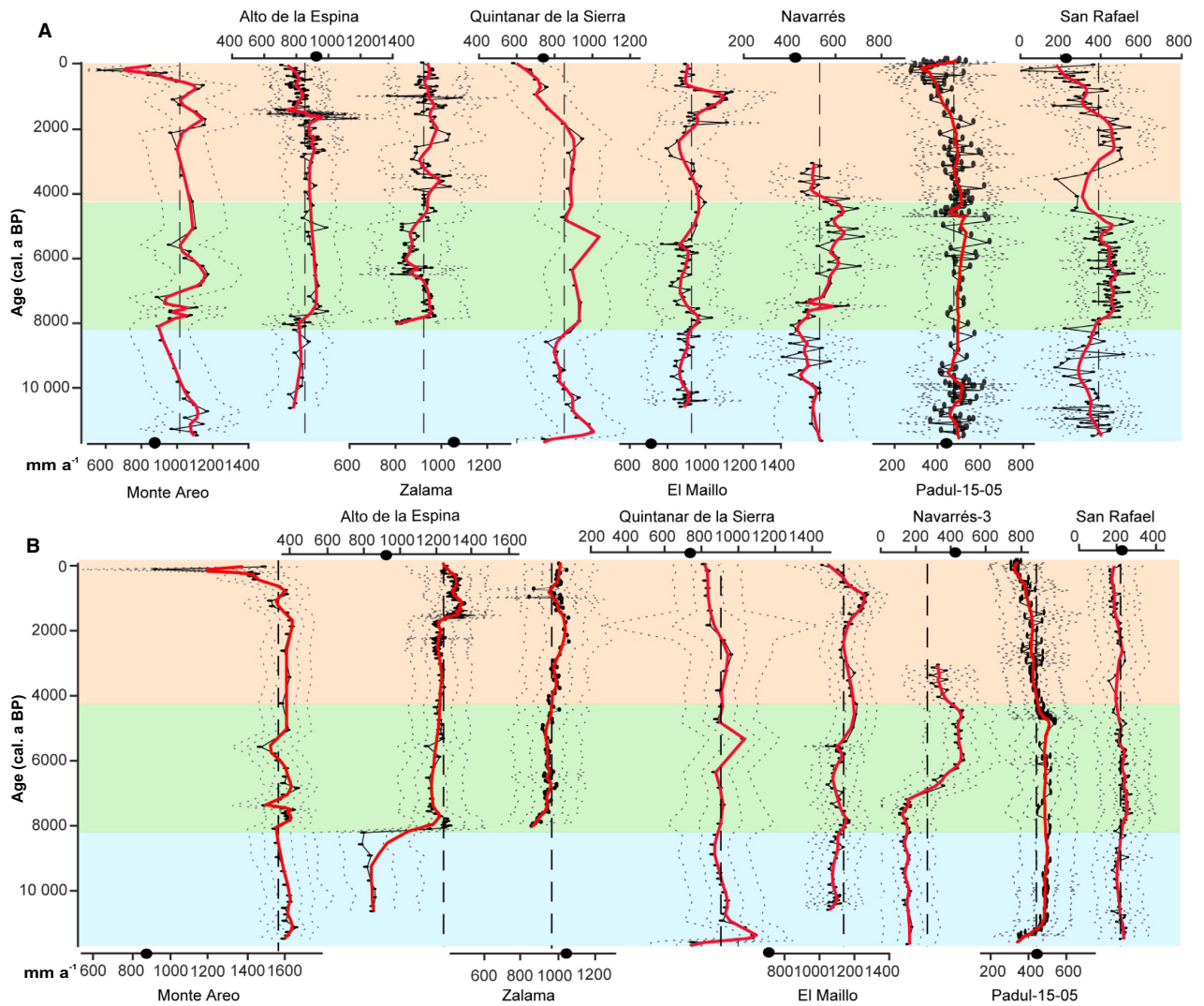


Fig. 4. P_{ann} (mm a^{-1}) reconstructions for eight pollen records using WAPLS (A) and Bayesian model (B). In (A) the black dots connected with the solid black line are the reconstructed values for P_{ann} , the solid red line is a LOWESS smoother added to the reconstructions (span 0.1) and the black dotted lines denote bootstrap estimated standard errors. In (B) the black dots connected with the solid black line are the posterior mean values for P_{ann} and the solid red line is a LOWESS smoother added to the reconstructions (span 0.1). The inner and outer black dotted lines show the point-wise and simultaneous 95% credible bands, respectively. In (A) and (B) the vertical stippled line indicates the mean value of each reconstruction. The big black dot is the modern measured value for P_{ann} . The x -axis is P_{ann} and the y -axis is time in years before present. Blue, green and orange shading indicate the formal stratigraphical subdivision of the Holocene (Walker *et al.* 2018).

with a limited number of lakes and peat bogs (Pontevedra-Pombal *et al.* 2017). We also tested our WAPLS calibration model for the possible spatial autocorrelation using the h -block test (Telford & Birks 2009). When the h -value is set at 20 km, the RMSEP increases to 170 mm and the R^2 decreases to 0.48. With this 20 km radius an average of 5.5 sites (min = 1, max = 20) were omitted in the h -block runs. This indicates some spatial autocorrelation in our calibration model. This is probably inevitable in a dataset such as ours, which is based on moss polster samples often collected from sites near each other.

Evaluation of the reconstructions

When the shapes of the reconstructions based on WAPLS and Bayesian modelling are compared, it can be seen that they are mostly comparable but the actual levels of reconstructed P_{ann} values may differ to some extent (Figs 4, S4). In general, the variability is higher in the WAPLS-based reconstructions, as can be seen especially in the records from Monte Aereo, San Rafael and El Maíllo, while the absolute reconstructed P_{ann} values are similar in both reconstruction approaches. Alto de la Espina is the only record where the main

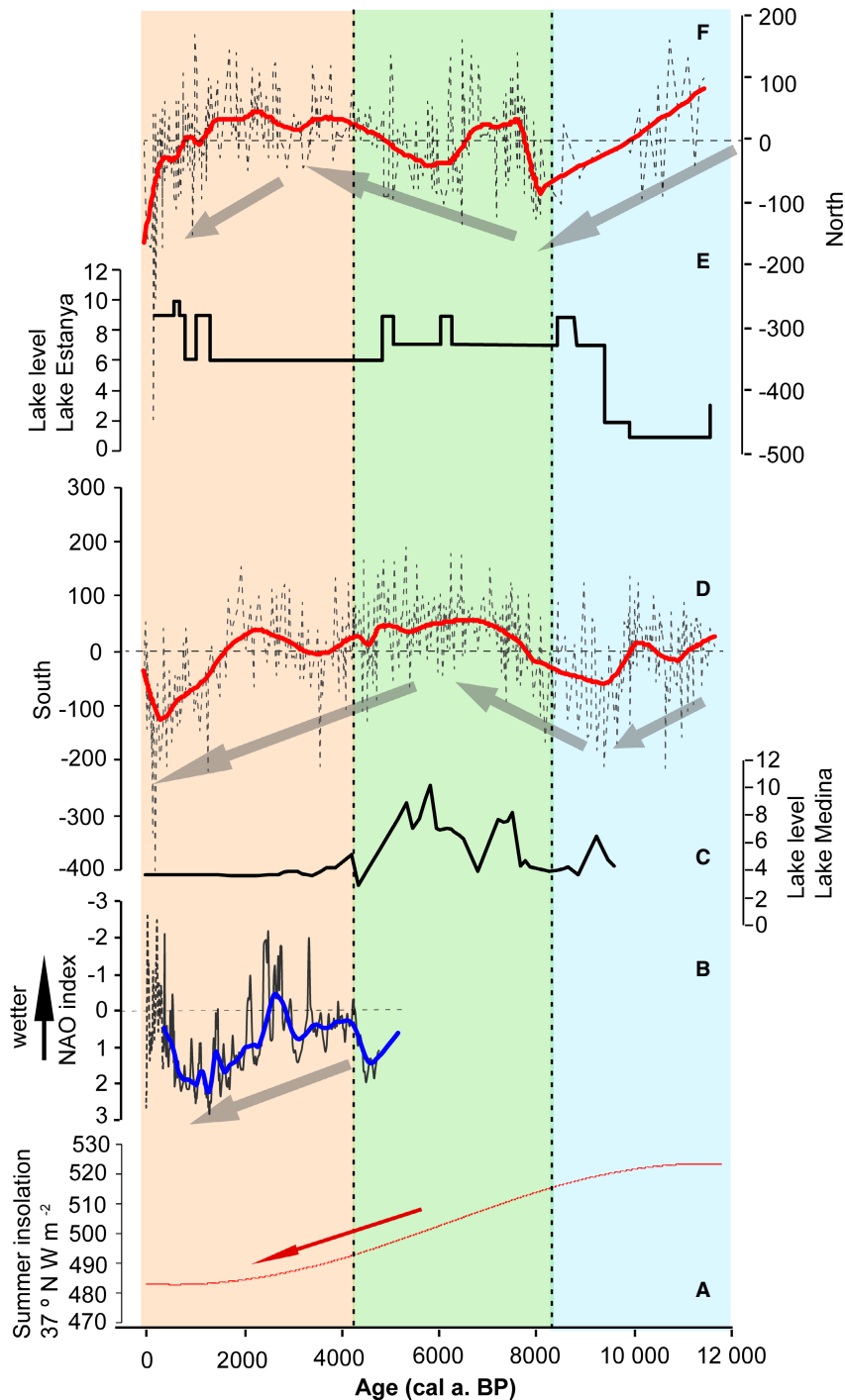


Fig. 5. A. Summer insolation from 37°N (Laskar *et al.* 2004). B. North-Atlantic Oscillation index reconstructions (Trouet *et al.* 2009; Olsen *et al.* 2012). C. Lake-level reconstruction of lake Medina (Schröder *et al.* 2018). D. Stack from the south of the Iberian Peninsula (this study). E. Lake-level reconstruction of lake Estanya (Morellón *et al.* 2009). F. Stack from the north of the Iberian Peninsula (this study).

features of the two reconstruction techniques are different (Figs 4, S4). For exploring the generality of our results, we compare them with selected Holocene lake-level records that reflect general humidity in the Iberian Peninsula. Additionally, to gain insights into the

underlying climatic mechanisms and climatic teleconnections that can explain the reconstructed features, we compare the results with a NAO reconstruction which represents Late Holocene climatic conditions in the North Atlantic region and the western Mediterranean region.

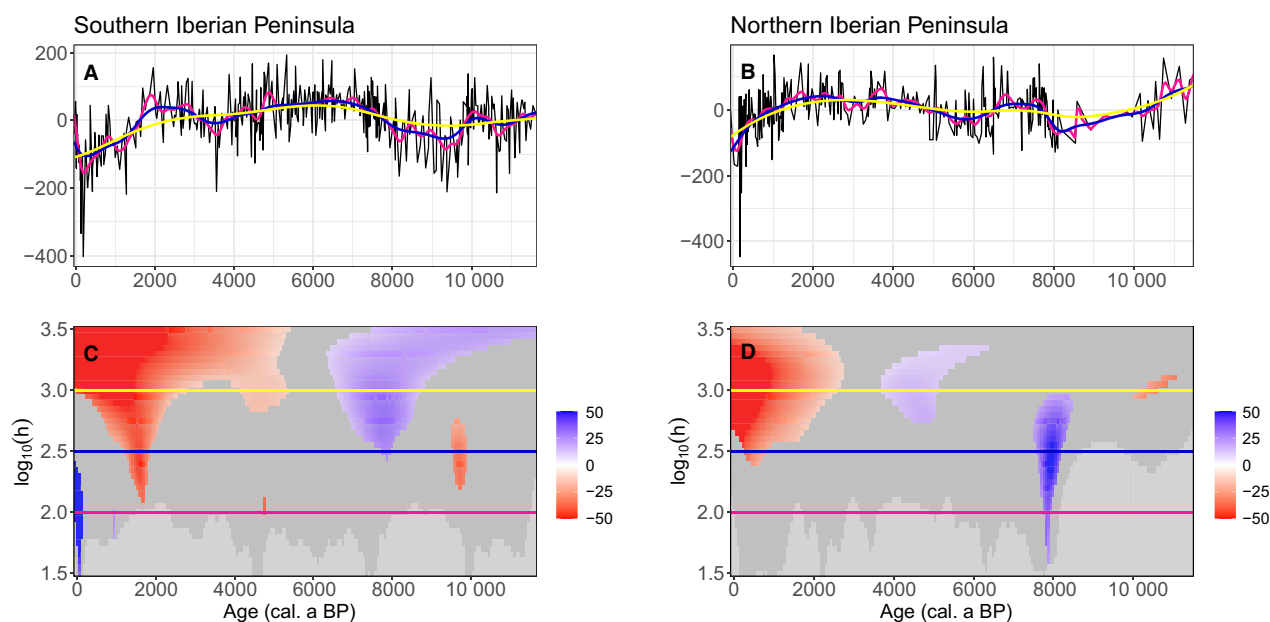


Fig. 6. The colour-enhanced SiZer analysis of the stack of northern Iberian Peninsula and southern Iberian Peninsula. In the upper panels (A and B) are stacks with three smooths each corresponding to different time scales for smoothing. Roughly speaking, the pink line shows multidecadal, blue centennial and yellow millennial variations in the deviations from the mean P_{ann} (mm a^{-1}) of each core. In the maps (lower panels C and D), the horizontal axis represents the time, the vertical axis the level of smoothing in logarithmic units and the colour of each pixel indicates significant increases and decreases in the P_{ann} at given time and level of smoothing. Blue indicates a significant increase in P_{ann} and red a significant decrease in P_{ann} as we read the data from past to present. Dark grey indicates absence of statistically significant features, and light grey indicates that the data are too sparse for inferences. The intensity of the colour indicates the magnitude of the precipitation change. Pink, blue and yellow horizontal lines are the smoothing levels corresponding to the three smooths from the upper panel.

Precipitation trends

A general feature of our reconstructions is the high P_{ann} values and thus humid conditions in the earliest Holocene both in the Atlantic and the Mediterranean regions, as can be seen in the reconstructed values in the Monte Aro, Quintanar de la Sierra, San Rafael and Navarrés-3 records (Figs 4, S3). The subsequent declining trend is stronger in the Atlantic region but can be seen in the Mediterranean region as well. These patterns are not fully compatible with the lake-level reconstruction data. For example, in the reconstruction from Estanya Lake, located in the transitional area between the Pyrenees and the semi-arid Central Ebro Basin in northeastern Spain, the Early Holocene (~11 600 to 9400 cal. a BP; Fig. 5) was characterized by shallow, ephemeral, saline lake–mud flat complex with carbonate-dominated sedimentation during the flooding episodes and gypsum precipitation during desiccation phases, thus suggesting generally low lake levels (Morellón *et al.* 2009). In the south, a humidity reconstruction based on speleothem data in Cueva Victoria in south-eastern Spain displays a strong positive excursion of the $\delta^{13}\text{C}$ values at 9700 to 7800 cal. a BP, interpreted as suggesting a major summer drought but an increase in fall/winter precipitation (Budsky *et al.* 2019). This period has been shown as the wettest in southern Iberian and the Mediterranean region (Dormoy *et al.* 2009; Anderson *et al.* 2011; Fletcher & Zielhofer 2013),

however the maximum in summer insolation produced a high summer evaporation effect that is reflected in low lake levels, like in Padul (Ramos-Román *et al.* 2018a) and Estanya lakes (Jiménez-Moreno & Anderson 2012; García-Alix *et al.* 2021). This roughly agrees with the period of lower P_{ann} in our southern Iberian stack (Fig. 5).

Our P_{ann} reconstructions and the lake-level data generally agree during the Middle Holocene humid period after 8000 cal. a BP. In northern Iberian Peninsula, in addition to high stand of Lake Estanya from 8000 to 4000 cal. a BP (Fig. 5), the reconstruction from Basa de la Mora Lake shows a period of highest Holocene lake levels from 8100 to 5700 cal. a BP (Pérez-Sanz *et al.* 2013; González-Sampérez *et al.* 2017). In southern Iberian Peninsula, a lake-level reconstruction from Laguna de Medina in south-western Spain suggests a humidity maximum at 7000–6000 cal. a BP, followed by a steady decline (Reed *et al.* 2001), and in a more detailed reinvestigation of the same lake, a period of highest lake level was observed at 7800 to 5000 cal. a BP (Schröder *et al.* 2018; Fig. 5). The period of highest lake level in the Padul-15-05 record also occurred in the Middle Holocene from around 7500 to 5500 cal. a BP (Ramos-Román *et al.* 2018a). This is mostly compatible with the reconstructed trend in Navarrés-3, Padul-15-05 and San Rafael, our southernmost records (Fig. 4). Thus, in most records in southern Spain the maximum humidity occurs after 8000 cal. a BP, until an abrupt shift

towards drier conditions at 5000 cal. a BP. In general, the comparisons of pollen-based precipitation reconstructions, lake-level records, biomarker data and speleothem isotope data show many consistent features in the Middle Holocene, but also differences that show that more detailed work is still needed to understand the timing and possible seasonal patterns in the Early to Middle Holocene humidity maximum in southern Spain.

An increasing dryness over the last 5000 years, evident in our P_{ann} records (Figs 4, S3, Table S3), has been observed in many records from the Iberian Peninsula. In the Basa de la Mora record, the lake level falls from 6000 to 4000 cal. a BP, with the period of lowest Holocene level from 3500 to 2300 cal. a BP, followed by a slight rise over the last two millennia (González-Sampéris *et al.* 2017). In the Estanya Lake record, more saline and shallower conditions are seen between 4800 and 1200 cal. a BP, as indicated by the deposition of gypsum-rich sediment and massive sapropels facies (Morellón *et al.* 2009). Similarly, the multiproxy data from the Padul-15-05 record in Sierra Nevada in Southern Spain show clear evidence for aridification over the last 4000 years (Ramos-Román *et al.* 2018b). A similar marked Late Holocene aridity trend is also indicated in the analysis of the isotopic composition of isolated *Cedrus* pollen grains in the Middle Atlas Mountains in Morocco, 500 km south of our southernmost site San Rafael (Bell *et al.* 2019).

The decreasing trend during the Late Holocene in southern Spain is interrupted by a positive excursion around 2500 to 2000 cal. a BP, coinciding with negative values in the NAO reconstruction (Fig. 5). The NAO, which is usually defined by the difference in pressure between the Azores (high) and Icelandic (low) controlling the latitudinal situation of the winter storm track (Visbeck *et al.* 2001), is currently, the main climatic system driving precipitation in the North Atlantic and the western Mediterranean regions. Nowadays, during positive NAO phases, higher differences are predominant between the low and high pressures, producing drier and colder conditions over the Mediterranean region while wetter and warmer conditions occur over northern Europe, and inversely during negative NAO conditions (Visbeck *et al.* 2001; Hernández *et al.* 2020). In addition, its impact on the climate of the Iberian Peninsula can be modulated by the Mediterranean Dipole Mode (Ortiz-Bevia *et al.* 2016), especially during the summer. During recent decades several studies have provided millennial-scale reconstructions of past NAO conditions (Trouet *et al.* 2009; Olsen *et al.* 2012; Baker *et al.* 2015) and NAO variability has been associated with humid and drier periods in the Iberian Peninsula (Martín-Puertas *et al.* 2009; Moreno *et al.* 2012; Ramos-Román *et al.* 2016; Hernández *et al.* 2020).

A characteristic feature in our P_{ann} reconstructions is a high variability in the records and between the records during the last 2000 years. The drop in reconstructed

P_{ann} from 1500 mm to under 600 mm during the last 500 years in the Monte Aro record is an extreme example of this pattern. It is possible that these rapid changes reflect the dynamics of NAO in the Iberian Peninsula over the last two millennia (Hernández *et al.* 2020), but it is more likely that these wiggles do not represent realistic changes in the P_{ann} values, but reflect more likely noise in the data. One reason for such variability may be the increasing human impact on vegetation in the Iberian Peninsula. Human impact has a long Holocene history in the Iberian Peninsula, and the earliest evidence of agriculture is documented in the eastern part of Spain as early as 7500 cal. a BP, during the Early Neolithic, after which agriculture spread across the peninsula (Peña-Chocarro *et al.* 2018).

In general, the pollen-based climate reconstructions in the Atlantic and Mediterranean regions are in most cases strongly influenced by the human impact on vegetation, including cultivation, forestry, husbandry, burning and clear cutting (Carrión *et al.* 2010; López-Merino *et al.* 2014; Lillios *et al.* 2016; Roberts *et al.* 2019). Over the centuries, human influence has caused the original natural vegetation to shift towards semi-anthropogenic ecosystems, creating novel plant communities such as olive (Ramos-Román *et al.* 2019), chestnut, walnut and cork-oak woodlands, or has promoted disturbance-adapted sclerophyllous vegetation types.

Short-lived events

A prerequisite for detecting the short-lived events in Holocene palaeoclimate records is that the temporal resolution of the records is adequately high. This is not the case with most of the individual records in our dataset and hence it is essential to use the stacks for analysing statistically the evidence of any events in the data. Our stacks have an average temporal resolution of 60 years and they should thus have adequate time resolution for analysing multicentennial and even subcentennial events. The 8.2 ka event is the clearest short-lived abrupt event in the Holocene records in the North Atlantic-northern European region (Alley *et al.* 1997) and evidence for this event has been suggested in many pollen records from the Iberian Peninsula (López-Sáez *et al.* 2008). On the Mediterranean coast and in the middle Ebro valley, it is characterized by the increase in Mediterranean pine and evergreen oak forests and the decline in deciduous oak (Davis & Stevenson 2007), while in the eastern part of the Iberian Peninsula (e.g. Les Alcusses and Navarrés; Fig. S1) the high-mountain pine forests are more adapted to a cold continental climate expanded, while the Mediterranean vegetation in lower and inner areas is reduced (Carrión & van Geel 1999; Tallón *et al.* 2014). Changes in lake level also indicate increased aridity, with desiccation during this period at Medina Lake in the south-west (Reed *et al.* 2001) and at Villafáfila lakes in inland Iberia (López-Sáez *et al.* 2017).

Given this background, it is notable that the SiZer analysis of the two stacks does not show any statistically significant evidence of lower P_{ann} values during the event. When we explore the individual records, we can see that in the Alto de la Espina record the reconstructed P_{ann} drops to under 800 mm at 8000 to 7900 cal. a BP, and in the Quintanar de la Sierra and San Rafael records there is a dip between 8300 and 8100 cal. a BP, but it is indicated only by one data point (Fig. 4). Thus, the reason for the lack of statistically significant evidence for the event is either that the time resolution in our data is still not sufficient or that the magnitude of the event was too low to be detected in our data. The other suggested main drought event may have taken place at 4200 cal. a BP (Bini *et al.* 2019), but our data do not show any evidence of a P_{ann} reduction during this period. Thus, there is no statistically unequivocal evidence for the 8.2 or 4.2 ka events in our data, but we cannot exclude their occurrence in the Iberian Peninsula either. We therefore conclude that at least where pollen-based records are considered, the occurrence of these events remains ambiguous and accurately dated high-resolution pollen records combined with statistical event detection analysis are needed to firmly and objectively detect the nature of these events.

Conclusions

Precipitation is a key driver for the ecosystems in the Iberian Peninsula and changes in its amount and spatial and temporal distributions have an impact on vegetation history, human activities and natural hazards. It is thus an important variable in climate and palaeoclimate studies. Thus far most of the reconstructions of changes in past precipitation in the Iberian Peninsula have been based on qualitative and indirect data, such as inferred vegetation changes or changes in lake levels. We have constructed a modern pollen–climate calibration set specifically for the Iberian Peninsula and used it to provide quantitative precipitation reconstructions from eight fossil pollen cores from different climatic regions. In general, the results show that precipitation in the Iberian Peninsula has had a strong spatial and latitudinal gradient during the last 12 000 years. The reconstructed P_{ann} values are clearly higher in northern Spain than at the three sites in the Mediterranean region. The most pronounced period with high P_{ann} values dates to 8000–6000 cal. a BP, and it is more clearly expressed in the records from the southern part of the peninsula. This humid period corresponds approximately with high lake levels in the southern part of the Iberian Peninsula. During the Late Holocene the reconstructions are less consistent with the precipitation decrease starting earlier in the south. One factor explaining this is probably the substantial human impact on vegetation, such as the clearance of forests and the development of cultivated fields, pastures, meadows and heathlands. The

pollen-based Late Holocene climate reconstructions from the Iberian Peninsula are thus substantially biased by the human impact.

Acknowledgements. – This research has been funded by the Academy of Finland (GRASS and HiDyn projects), by the European Research Council (project YMPACT), and through the REDISCO-HAR2017-88035-P (Plan Nacional I + D+I, Spanish Ministry of Economy and Competitiveness), RTI2018-101714-B-I00 (Spanish government), B-RNM-404-UGR18 (ERDF-Andalusian Government) and P18-RT-4963 (Andalusian Government). Pollen data were extracted from the European Pollen Database (EPD; <http://www.europeanpollendatabase.net/>) and the work of the data contributors and the EPD community is gratefully acknowledged. We thank the two reviewers (T. Schröder and an anonymous reviewer) and Jan A. Piotrowski (editor-in-chief) for their constructive comments and suggestions, which improved the quality of the manuscript.

Author contributions. – LI, JALS and HS designed the study. LI performed the simulations and computations required for the Bayesian model and WAPLS method. JALS, FAS, SPD, JSC, MJRR and JCB provided the data. LR provided the modified code to perform the colour-enhanced SiZer analyses. LI, JALS and HS were mainly responsible for preparing the manuscript, while all authors commented and contributed to the discussion and interpretations. The authors declare that they have no conflict of interest.

Data availability statement. – Code used to conduct the analysis for the Bayesian model has been published in *The Annals of Applied Statistics* as Holmström *et al.* (2015): <https://doi.org/10.1214/15-AOAS832SUPPC>. In order to run the model used in this manuscript the prior distributions need to be set according to Table S2. The information about modern pollen samples is as Table S1. Other data are available from the authors upon request.

References

- Alba-Sánchez, F., Abel-Schaad, D., López-Sáez, J. A., Sabariego-Ruiz, S., Pérez-Díaz, S., Luelmo-Lautenschlaeger, R. & Garrido-García, J. A. 2021: Early anthropogenic change in western Mediterranean mountains (Sierra Nevada, SE Spain). *Anthropocene* 33, 100278. <https://doi.org/10.1016/j.ancene.2021.100278>.
- Alley, R. B., Mayewski, P. A., Sowers, T., Stuiver, M., Taylor, K. C. & Clark, P. U. 1997: Holocene climate instability: a prominent, widespread event 8200 yr ago. *Geology* 25, 483–486.
- Anderson, R. S., Jiménez-Moreno, G., Carrión, J. S. & Pérez-Martínez, C. 2011: Postglacial history of alpine vegetation, fire, and climate from Laguna de Río Seco, Sierra Nevada, southern Spain. *Quaternary Science Reviews* 30, 1615–1629.
- Baker, A., Hellstrom, J. C., Kelly, B. F. J., Mariethoz, G. & Trouet, V. 2015: A composite annual-resolution stalagmite record of North Atlantic climate over the last three millennia. *Scientific Reports* 5, 10307.
- Bell, B. A., Fletcher, W. J., Cornelissen, H. L., Campbell, J. F. E., Ryan, P., Grant, H. & Zielhofer, C. 2019: Stable carbon isotope analysis on fossil *Cedrus* pollen shows summer aridification in Morocco during the last 5000 years. *Journal of Quaternary Science* 34, 323–332.
- Benito-Garzón, M., Sánchez de Dios, R. & Sainz Ollero, H. 2008: Effects of climate change on the distribution of Iberian tree species. *Applied Vegetation Science* 11, 169–178.
- Bini, M., Zanchetta, G., Perşoiu, A., Cartier, R., Català, A., Cacho, I., Dean, J. R., Di Rita, F., Drysdale, R. N., Finnè, M., Isola, I., Jalali, B., Lirer, F., Magri, D., Masi, A., Marks, L., Mercuri, A. M., Peyron, O., Sadori, L., Sicre, M. A., Welc, F., Zielhofer, C. & Brisset, E. 2019: The 4.2 ka BP Event in the Mediterranean region: an overview. *Climate of the Past* 15, 135–151. <https://doi.org/10.5194/cp151352019>.
- Birks, H. J. B. 1995: Quantitative palaeoenvironmental reconstructions. Statistical Modelling of Quaternary Science Data. *Technical Guide* 5, 161–254.

- Birks, H. J. B. & Seppä, H. 2004: Pollen-based reconstructions of late-Quaternary climate in Europe – progress, problems, and pitfalls. *Acta Palaeobotanica* 44, 317–334.
- Birks, H. J. B., Heiri, O., Seppä, H. & Bjune, A. E. 2010: Strengths and weaknesses of quantitative climate reconstructions based on late-Quaternary biological proxies. *The Open Ecology Journal* 3, 68–110.
- Birks, H. J. B., Line, J., Juggins, S., Stevenson, A. & Ter Braak, C. 1990: Diatoms and pH reconstruction. *Philosophical Transactions of the Royal Society B, Biological Sciences* 327, 263–278.
- Blanco-Castro, E., Casado, M. A., Costa, M., Escribano, R., García-Antón, M., Génova, M., Gómez-Manzanaque, A., Gómez-Manzanaque, F., Moreno, J. C., Morla, C., Regato, P. & Sainz-Ollero, H. 1997: *Los bosques ibéricos. Una interpretación geobotánica*. 572 pp. Planeta, Barcelona.
- Blanco-González, A., Lillios, K. T., López-Sáez, J. A. & Drake, B. L. 2018: Cultural, demographic and environmental dynamics of the Copper and Early Bronze Age in Iberia (3300–1500 BC): towards an interregional multiproxy comparison at the time of the 4.2 ky BP event. *Journal of World Prehistory* 31, 1–79.
- Blondel, J., Aronson, J., Bodiou, J. Y. & Boeuf, G. 2010: *The Mediterranean Region: Biological Diversity through Time and Space*. 376 pp. Oxford University Press, Oxford.
- ter Braak, C. J. & Juggins, S. 1993: Weighted averaging partial least squares regression (WA-PLS): an improved method for reconstructing environmental variables from species assemblages. *Hydrobiologia* 269, 485–502.
- Budsky, A., Scholz, D., Wassenburg, J. A., Mertz-Kraus, R., Spötl, C., Riechelmann, D. F. C., Gibert, L., Jochum, K. P. & Andreae, M. O. 2019: Speleothem $\delta^{13}\text{C}$ record suggests enhanced spring/summer drought in south-eastern Spain between 9.7 and 7.8 ka – A circum-Western Mediterranean anomaly? *The Holocene* 29, 1113–1133.
- Camuera, J., Jiménez-Moreno, G., Ramos-Román, M. J., García-Alix, A., Toney, J. L., Anderson, R. S., Jiménez-Espejo, F., Kaufman, D., Bright, J., Webster, C., Yanes, Y., Carrión, J. S., Ohkouchi, N., Suga, H., Yamame, M., Yokoyama, Y. & Martínez-Ruiz, F. 2018: Orbital-scale environmental and climatic changes recorded in a new ~200,000-year-long multiproxy sedimentary record from Padul, southern Iberian Peninsula. *Quaternary Science Reviews* 198, 91–114.
- Capel, J. J. 2000: *El clima de la península ibérica*. 282 pp. Ariel, Barcelona.
- Carrión, J. S. (ed.) 2015: *Cinco millones de años de cambio florístico y vegetal en la Península Ibérica e Islas Baleares*. 1017 pp. Ministerio de Economía y Competitividad, Madrid.
- Carrión, J. S. & van Geel, B. 1999: Fine-resolution Upper Weichselian and Holocene palynological record from Navarrés (Valencia, Spain) and a discussion about factors of Mediterranean forest succession. *Review of Palaeobotany and Palynology* 106, 209–236.
- Carrión, J. S., Fernández, S., González-Sampériz, P., Gil-Romera, G., Badal, E., Carrión-Marco, Y., López-Merino, L., López-Sáez, J. A., Fierro, E. & Burjachs, F. 2010: Expected trends and surprises in the Lateglacial and Holocene vegetation history of the Iberian Peninsula and Balearic Islands. *Review of Palaeobotany and Palynology* 162, 458–475.
- Carrión, J. S., Munuera, M., Navarro, C. & Sáez, F. 2000a: Paleoclimase historia de la vegetación cuaternaria en España a través del análisis polínico. *Viejas falacias y nuevos paradigmas, Complutum* 11, 115–142.
- Carrión, J. S., Parra, I. & Navarro, C. 2000b: The past distribution and ecology of the cork oak (*Quercus suber*) in the Iberian Peninsula: a pollen-analytical approach. *Diversity and Distributions* 6, 29–44.
- Chaudhuri, P. & Marron, J. S. 1999: SiZer for exploration of structures in curves. *Journal of the American Statistical Association* 94, 807–823.
- Chevalier, M., Davis, B. A. S., Heiri, O., Seppä, H., Chase, B. M., Gajewski, K., Lacourse, T., Telford, R. J., Finsinger, W., Guiot, J., Kühl, N., Maezumi, S. Y., Tipton, J. R., Carter, V. A., Brussel, T., Phelps, L. N., Dawson, A., Zanon, M., Vallé, F., Nolan, C., Mauri, A., de Vernal, A., Izumi, K., Holmström, L., Marsicek, J., Goring, S., Sommer, P. S., Chaput, M. & Kupriyanov, D. 2020: Pollen-based climate reconstruction techniques for late Quaternary studies. *Earth-Science Reviews* 210, 103384, <https://doi.org/10.1016/j.earscirev.2020.103384>.
- Clements, W. H. & Rohr, J. R. 2009: Community responses to contaminants: Using basic ecological principles to predict ecotoxicological effects. *Environmental Toxicology and Chemistry* 28, 1789–1800.
- Clements, W. H., Vieira, N. K. M. & Sonderegger, D. L. 2010: Use of ecological thresholds to assess recovery in lotic ecosystems. *Journal of the North American Benthological Society* 29, 1017–1023.
- Combourieu-Nebout, N., Peyron, O., Dormoy, I., Desprat, S., Beaudouin, C., Kotthoff, U. & Marret, F. 2009: Rapid climatic variability in the west Mediterranean during the last 25 000 years from high resolution pollen data. *Climate of the Past* 5, 503–521.
- Dasari, H. P., Pozo, I., Ferri-Yáñez, F. & Araújo, M. B. 2014: A regional climate study of heat waves over the Iberian Peninsula. *Atmospheric and Climate Sciences* 4, 841–853.
- Davis, B. A. S. & 69 others 2013: The European Modern Pollen Database (EMPD) project. *Vegetation History and Archaeobotany* 22, 521–530.
- Davis, B. A. & 100 others 2020: The Eurasian Modern Pollen Database (EMPD), version 2. *Earth system science data* 12, 2423–2445.
- Davis, B. A. S. & Stevenson, A. C. 2007: The 8.2 ka event and Early-Mid Holocene forests, fires and flooding in the Central Ebro Desert, NE Spain. *Quaternary Science Reviews* 26, 1695–1712.
- Divine, D. V., Isaksson, E., Kaczmarek, M., Godtliebsen, F., Oerter, H., Schlosser, E., Johnsen, S. J., Van Den Broeke, M. & Van DeWal, R. S. W. 2009: Tropical Pacific–high latitude south Atlantic teleconnections as seen in i180 variability in Antarctic coastal ice cores. *Journal of Geophysical Research: Atmospheres* 114, D11112.
- Dormoy, I., Peyron, O., Combourieu Nebout, N., Goring, S., Kotthoff, U., Magny, M. & Pross, J. 2009: Terrestrial climate variability and seasonality changes in the Mediterranean region between 15 000 and 4000 years BP deduced from marine pollen records. *Climate of the Past* 5, 615–632.
- Dükeloh, A. & Jacobeit, J. 2003: Circulation dynamics of Mediterranean precipitation variability 1948–1998. *International Journal of Climatology: A Journal of the Royal Meteorological Society* 23.15, 1843–1866.
- Erästä, P., Holmström, L., Korhola, A. & Weckström, J. 2012: Finding a consensus on credible features among several paleoclimate reconstructions. *Annals of Applied Statistics* 6, 1377–1405.
- Erästä, P. & Holmström, L. 2006: Prior selection and multiscale analysis in Bayesian temperature reconstruction based on species assemblages. *Journal of Paleolimnology* 36, 69–80.
- Fick, S. E. & Hijmans, R. J. 2017: WorldClim 2: new 1-km spatial resolution climate surfaces for global land areas. *International Journal of Climatology* 37, 4302–4315.
- Fletcher, W. J., Sánchez Goñi, M. F., Peyron, O. & Dormoy, I. 2010: Abrupt climate changes of the last glaciation detected in a Western Mediterranean forest record. *Climate of the Past* 6, 245–264.
- Fletcher, W. J. & Zielhofer, C. 2013: Fragility of Western Mediterranean landscapes during Holocene rapid climate changes. *Catena* 103, 16–29.
- García-Alix, A., Camuera, J., Ramos-Román, M. J., Toney, J. L., Sachse, D., Schefuß, E., Jiménez-Moreno, G., Jiménez-Espejo, F. J., López-Avilés, A., Anderson, R. S. & Yanes, Y. 2021: Paleohydrological dynamics in the Western Mediterranean during the last glacial cycle. *Global and Planetary Change* 202, 103527, <https://doi.org/10.1016/j.gloplacha.2021.103527>.
- Giorgi, F. & Lionello, P. 2008: Climate change projections for the Mediterranean region. *Global and Planetary Change* 63, 90–104.
- Godtliebsen, F., Holmström, L., Miettinen, A., Erästä, P., Divine, D. V. & Koc, N. 2012: Pairwise scale space comparison of time series with application to climate research. *Journal of Geophysical Research: Oceans* 117, C03046.
- González-Sampériz, P., Aranbarri, J., Pérez-Sáenz, A., Gil-Romera, G., Moreno, A., Leunda, M., Sevilla-Callejo, M., Corella, J. P., Morellón, M., Oliva, B. & Valero-Garcés, B. L. 2017: Environmental and climate change in the southern Central Pyrenees since the Last Glacial Maximum: A view from the lake records. *Catena* 149, 668–688.
- Haslett, J. & Parnell, A. 2008: A simple monotone process with application to radiocarbon-dated depth chronologies. *Journal of the Royal Statistical Society: Series C (Applied Statistics)* 57, 399–418.

- Hernández, A., Sánchez-López, G., Pla-Rabes, S., Comas-Bru, L., Parnell, A., Cahill, N., Geyer, A., Trigo, R. M. & Giral, S. 2020: A 2,000-year Bayesian NAO reconstruction from the Iberian Peninsula. *Scientific Reports* 10, 14961, <https://doi.org/10.1038/s41598-020-71372-5>.
- Holmström, L., Ilvonen, L., Seppä, H. & Veski, S. 2015: A Bayesian spatiotemporal model for reconstructing climate from multiple pollen records. *The Annals of Applied Statistics* 9, 1194–1225.
- Jiménez-Moreno, G. & Anderson, R. S. 2012: Holocene vegetation and climate change recorded in alpine bog sediments from the Borreguiles de la Virgen, Sierra Nevada, southern Spain. *Quaternary Research* 77, 44–53.
- Jiménez-Moreno, G., Rodríguez-Ramírez, A., Pérez-Asensio, J. N., Carrión, J. S., López-Sáez, J. A., Villarias-Robles, J. J. R., Celestino-Pérez, S., Cerrillo-Cuenca, E., León, A. & Contreras, C. 2015: Impact of late-Holocene aridification trend, climate variability and geodynamic control on the environment from a coastal area in SW Spain. *The Holocene* 25, 607–617.
- Juggins, S. 2007: *C2: Software for Ecological and Palaeoecological Data Analysis and Visualisation (User Guide Version 1.5)*. Newcastle University, Newcastle upon Tyne.
- Juggins, S. & Birks, H. J. B. 2012: Quantitative environmental reconstructions from biological data, in: Tracking Environmental Change Using Lake Sediments. In Birks, H. J. B., Lotter, A. F., Juggins, S. & Smol, J. (eds.): *Developments in Paleoenvironmental Research* 5, 431–494. Springer, Dordrecht.
- Karagiannidis, A. F., Bloutsos, A. A., Maheras, P. & Sachsamanoglou, C. 2008: Some statistical characteristics of precipitation in Europe. *Theoretical and Applied Climatology* 91, 193–204.
- Korhola, A., Weckström, J., Holmström, L. & Erästö, P. 2000: A quantitative Holocene climatic record from diatoms in northern Fennoscandia. *Quaternary Research* 54, 284–294.
- Laskar, J., Robutel, P., Joutel, F., Gastineau, M., Correia, A. C. M. & Levrard, B. 2004: A long term numerical solution for the insolation quantities of the Earth. *Astronomy & Astrophysics* 428, 261–285.
- Li, J., Ilvonen, L., Xu, Q., Ni, J., Jin, L., Holmström, L., Cao, X., Zheng, Z., Lu, H., Luo, Y., Li, Y., Li, C., Zhang, X. & Seppä, H. 2016: East Asian summer monsoon precipitation variations in monsoonal China over the last 9500 years: a comparison of pollen-based reconstructions and model simulations. *The Holocene* 26, 592–602.
- Li, J., Xu, Q., Zheng, Z., Lu, H., Luo, Y., Li, Y., Li, C., Huang, K., Luo, C., Zheng, Y. & Seppä, H. 2015: Assessing the relative importance of climatic variables for the spatial distribution patterns of pollen taxa in China. *Quaternary Research* 83, 287–297.
- Lillios, K. T., Blanco-González, A., Drake, B. L. & López-Sáez, J. A. 2016: Mid-Late Holocene climate, demography, and cultural dynamics in Iberia: a multi-proxy approach. *Quaternary Science Reviews* 135, 138–153.
- Lindeberg, T. 1998: Feature detection with automatic scale selection. *International Journal of Computer Vision* 30, 79–116.
- Lionello, P., Malanotte-Rizzoli, P. & Boscoso, R. (eds.) 2006: *Mediterranean Climate Variability, vol 4*. 438 pp. Elsevier, Amsterdam.
- Loidi, J. (eds.) 2017: *The Vegetation of the Iberian Peninsula*. 676 pp. Springer, Berlin.
- López-Merino, L. 2009: *Paleoambiente y antropización en Asturias durante el Holoceno*. Ph.D. thesis. Universidad Autónoma de Madrid, 274 pp.
- López-Merino, L., Martínez-Cortizas, A. & López-Sáez, J. A. 2010: Early agriculture and palaeoenvironmental history in the North of the Iberian Peninsula: a multi-proxy analysis of the Monte Areo mire (Asturias, Spain). *Journal of Archaeological Science* 37, 1978–1988.
- López-Merino, L., Martínez-Cortizas, A. & López-Sáez, J. A. 2011: Human-induced changes on wetlands: a study case from NW Iberia. *Quaternary Science Reviews* 30, 2745–2754.
- López-Merino, L., Martínez-Cortizas, A., Reher, G. S., López-Sáez, J. A., Mighall, T. M. & Bindler, R. 2014: Reconstructing the impact of human activities in a NW Iberian Roman mining landscape for the last 2500 years. *Journal of Archaeological Science* 50, 208–218.
- López-Sáez, J. A., Abel-Schaad, D., Iriarte, E., Alba-Sánchez, F., Pérez-Díaz, S., Guerra, E., Delibes, G. & Abarquero, F. J. 2017: Una perspectiva paleoambiental de la explotación de la sal en las Lagunas de Villafáfila (Tierra de Campos, Zamora). *Cuaternario y Geomorfología* 31, 73–104.
- López-Sáez, J. A., Alba-Sánchez, F., López-Merino, L. & Pérez-Díaz, S. 2010: Modern pollen analysis: a reliable tool for discriminating *Quercus rotundifolia* communities in Central Spain. *Phytocoenologia* 40, 57–72.
- López-Sáez, J. A., Alba-Sánchez, F., Robles, S., Pérez-Díaz, S., Abel-Schaad, D., Sabariego, S. & Glais, A. 2016: Exploring seven hundred years of transhumance, climate dynamic, fire and human activity through a historical mountain pass in central Spain. *Journal of Mountain Science* 13, 1139–1153.
- López-Sáez, J. A., Alba-Sánchez, F., Sánchez-Mata, D., Abel-Schaad, D., Gavilán, R. G. & Pérez-Díaz, S. 2015: A palynological approach to the study of *Quercus pyrenaica* forest communities in the Spanish Central System. *Phytocoenologia* 45, 107–124.
- López-Sáez, J. A., Camarero, J. J., Abel-Schaad, D., Luelmo-Lautenschlaeger, R., Pérez-Díaz, S., Alba-Sánchez, F. & Carrión, J. S. 2020: Don't lose sight of the forest for the trees! Discerning Iberian pine communities by means of modern pollen-vegetation relationships. *Review of Palaeobotany and Palynology* 281, 104285, <https://doi.org/10.1016/j.revpalbo.2020.104285>.
- López-Sáez, J. A., López-Merino, L. & Pérez-Díaz, S. 2008: Crisis climáticas en la Prehistoria de la Península Ibérica: el evento 8200 cal. BP como modelo. In Rovira, S., García, M., Gener, M. & Montero, I. (eds.): *Actas VII Congreso Ibérico de Arqueometría*, 77–86. Publicación CCHS-IH, Madrid.
- López-Sáez, J. A., Sánchez-Mata, D., Alba-Sánchez, F., Abel-Schaad, D., Gavilán, R. G. & Pérez-Díaz, S. 2013: Discrimination of Scots pine forests in the Iberian Central System (*Pinus sylvestris* var. *iberica*) by means of pollen analysis. *Phytosociological considerations Lazaroa* 34, 191–208.
- Lotter, A. F., Birks, H. J. B., Eicher, U., Hofmann, W., Schwander, J. & Wick, L. 2000: Younger Dryas and Allerød temperatures at Gerzensee (Switzerland) inferred from fossil pollen and cladoceran assemblages. *Palaeogeography, Palaeoclimatology, Palaeoecology* 159, 349–361.
- Martín-Puertas, C., Valero-Garcés, B. L., Brauer, A., Mata, P. M., Delgado-Huertas, A. & Dulski, P. 2009: The Iberian-Roman humid period (2600–1600 cal yr BP) in the Zoñar Lake varve record (Andalucía, southern Spain). *Quaternary Research* 71, 108–120.
- Miettinen, A., Divine, D., Koç, N., Godtlielsen, F. & Hall, I. R. 2012: Multicentennial variability of the sea surface temperature gradient across the Subpolar North Atlantic over the last 2.8 kyr. *Journal of Climate* 25, 4205–4219.
- Moore, P. D., Webb, J. A. & Collinson, M. E. 1991: *Pollen Analysis*. 216 pp. Blackwell Scientific Publications, London.
- Morales-Molino, C., García-Antón, M., Postigo-Mijarra, J. M. & Morla, C. 2013: Holocene vegetation, fire and climate interactions on the westernmost fringe of the Mediterranean Basin. *Quaternary Science Reviews* 59, 5–17.
- Morellón, M., Aranbarri, J., Moreno, A., González-Sampérez, P. & Valero-Garcés, B. L. 2018: Early Holocene humidity patterns in the Iberian Peninsula reconstructed from lake, pollen and speleothem records. *Quaternary Science Reviews* 181, 1–18.
- Morellón, M., Valero-Garcés, B. L., Vegas-Villarrúbia, T., González-Sampérez, P., Romero, O., Delgado-Huertas, A., Mata, P., Moreno, A., Rico, M. & Corella, J. P. 2009: Lateglacial and Holocene palaeohydrology in the western Mediterranean region: the Lake Estanya record (NE Spain). *Quaternary Science Reviews* 28, 2582–2599.
- Moreno, A., Pérez, A., Frigola, J., Nieto-Moreno, V., Rodrigo-Gámiz, M., Martrat, B., González-Sampérez, P., Morellón, M., Martín-Puertas, C., Corella, J. P., Belmonte, A., Sancho, C., Cacho, I., Herrera, G., Canals, M., Grimalt, J. O., Jiménez-Espejo, F., Martínez-Ruiz, F., Vegas-Villarrúbia, T. & Valero-Garcés, B. L. 2012: The Medieval Climate Anomaly in the Iberian Peninsula reconstructed from marine and lake records. *Quaternary Science Reviews* 43, 16–32.
- Ninyerola, M., Pons, X. & Roure, J. M. 2007: Monthly precipitation mapping of the Iberian Peninsula using spatial interpolation tools implemented in a Geographic Information System. *Theoretical and Applied Climatology* 89, 195–209.

- Olsen, J., Anderson, N. J. & Knudsen, M. F. 2012: Variability of the North Atlantic Oscillation over the past 5,200 years. *Nature Geoscience* 5, 808–812.
- Olsen, L., Chaudhuri, P. & Godtliebsen, F. 2008: Multiscale spectral analysis for detecting short and long range change points in time series. *Computational Statistics and Data Analysis* 52, 3310–3330.
- Ortiz-Bevia, M. J., Ruiz-de-Elvira, A., Alvarez-Garcia, F. J. & Tasambay-Salazar, M. 2016: The multidecadal component of the Mediterranean summer variability. *Climate Dynamics* 47, 3373–3386.
- Pantaléon-Cano, J., Yll, E. I., Pérez-Obiol, R. & Roure, J. M. 2003: Palynological evidence for vegetational history in semi-arid areas of the western Mediterranean (Almería, Spain). *The Holocene* 13, 109–119.
- Parnell, A., Haslett, J., Sweeney, J., Doan, T., Allen, J. & Huntley, B. 2016: Joint palaeoclimate reconstruction from pollen data via forward models and climate histories. *Quaternary Science Reviews* 151, 111–126.
- Pasho, E., Camaero, J. J., de Luiz, M. & Vicente-Serrano, S. M. 2011: Impacts of drought at different time scales on forest growth across a wide climatic gradient in north-eastern Spain. *Agricultural and Forest Meteorology* 151, 1800–1811.
- Peña-Chocarro, L., Pérez-Jordà, G. & Morales, J. 2018: Crops of the first farming communities in the Iberian Peninsula. *Quaternary International* 470, 369–382.
- Peñalba, M. C. 1994: The history of the Holocene vegetation in northern Spain from pollen analysis. *Journal of Ecology* 82, 815–832.
- Peñalba, M. C., Arnold, M., Guiot, J., Duplessy, J. C. & de Beaulieu, J. L. 1997: Termination of the Last Glaciation in the Iberian Peninsula inferred from the pollen sequence of Quintanar de la Sierra. *Quaternary Research* 48, 205–214.
- Pérez-Díaz, S., López-Sáez, J. A., Pontevedra, X., Souto, M. & Galop, D. 2016: 8000 years of vegetation history in the northern Iberian Peninsula inferred from the palaeoenvironmental study of the Zalama ombrotrophic bog (Basque-Cantabrian Mountains, Spain). *Boreas* 45, 658–672.
- Pérez-Sanz, A., González-Sampériz, P., Moreno, A., Valero-Garcés, B. L., Gil-Romera, G., Rieradevall, M., Tarrats, P., Lasheras, L., Morellón, M., Belmonte, A., Sancho, C., Sevilla, M. & Navas, A. 2013: Holocene climate variability, vegetation dynamics and fire regime in the central Pyrenees: the Basa de la Mora sequence (NE Spain). *Quaternary Science Reviews* 73, 149–169.
- Pontevedra-Pombal, X., Castro, D., Carballeira, R., Souto, M., López-Sáez, J. A., Pérez-Díaz, S., Fraga, M. I., Valcárcel, M. & García-Rodeja, E. 2017: Iberian acid peatlands: types, origin and general trends of development. *Mires Peat* 19, 1–19.
- R Development Core Team 2020: R: *A Language and Environment for Statistical Computing*. Vienna: R Foundation for Statistical Computing. Available at: www.R-project.org.
- Ramos-Román, M. J., Jiménez-Moreno, G., Anderson, R. S., García-Alix, A., Camuera, J., Mesa-Fernández, J. M. & Manzano, S. 2019: Climate controlled historic olive tree occurrences and olive oil production in southern Spain. *Global and Planetary Change* 182, 102996. <https://doi.org/10.1016/j.gloplacha.2019.102996>.
- Ramos-Román, M. J., Jiménez-Moreno, G., Anderson, R. S., García-Alix, A., Toney, J. L., Jiménez-Espejo, F. J. & Carrion, J. S. 2016: Centennial-scale vegetation and north Atlantic oscillation changes during the late Holocene in the southern Iberia. *Quaternary Science Reviews* 143, 84–95.
- Ramos-Román, M. J., Jiménez-Moreno, G., Camuera, J., García-Alix, A., Anderson, R. S., Jiménez-Espejo, F. J. & Carrion, J. S. 2018b: Holocene climate aridification trend and human impact interrupted by millennial- and centennial-scale climate fluctuations from a new sedimentary record from Padul (Sierra Nevada, southern Iberian Peninsula). *Climate of the Past* 14, 117–137.
- Ramos-Román, M. J., Jiménez-Moreno, G., Camuera, J., García-Alix, A., Anderson, R. S., Jiménez-Espejo, F. J., Sachse, D., Toney, J. L., Carrion, J. S., Webster, C. & Yanes, Y. 2018a: Millennial-scale cyclical environment and climate variability during the Holocene in the western Mediterranean region deduced from a new multiproxy analysis from the Padul record (Sierra Nevada, Spain). *Global and Planetary Change* 168, 135–153.
- Reed, J. M., Stevenson, A. C. & Juggins, S. 2001: A multi-proxy record of Holocene climatic change in southwestern Spain: the Laguna de Medina, Cádiz. *The Holocene* 11, 707–719.
- Rivas-Martínez, S. 2007: Mapa de series, geoserias y geopermaseries de vegetación de España. Memoria del mapa de la vegetación potencial de España, parte 1. *Itinera Geobotanica* 17, 5–435.
- Roberts, N., Woodbridge, J., Palmisano, A., Bevan, A., Fyfe, R. & Shannon, S. 2019: Mediterranean landscape change during the Holocene: Synthesis, comparison and regional trends in population, land cover and climate. *The Holocene* 29, 923–937.
- Salonen, J. S., Ilvonen, L., Seppä, H., Holmström, L., Telford, R. J., Gaidamavičius, A., Stančičkaite, M. & Subetto, D. 2012: Comparing different calibration methods (WA/WA-PLS regression and Bayesian modelling) and different-sized calibration sets in pollen-based quantitative climate reconstruction. *The Holocene* 22, 413–424.
- Samartin, S., Heiri, O., Joos, F., Renssen, H., Franke, J., Brönnimann, S. & Tinner, W. 2017: Warm Mediterranean mid-Holocene summers inferred from fossil midge assemblages. *Nature Geoscience* 10, 207–212.
- Schröder, T. & van't Hoff, J., López-Sáez, J. A., Viehberg, F., Melles, M. & Reicherter, K. 2018: Holocene climatic and environmental evolution on the southwestern Iberian Peninsula: A high-resolution multi-proxy study from Lake Medina (Cadiz, SW Spain). *Quaternary Science Reviews* 198, 208–225.
- Seppä, H. & Bennett, K. D. 2003: Quaternary pollen analysis: recent progress in palaeoecology and palaeoclimatology. *Progress in Physical Geography* 27, 580–611.
- Seppä, H., Birks, H. J. B., Odland, A., Poska, A. & Veski, S. 2004: A modern pollen-climate calibration set from northern Europe: developing and testing a tool for palaeoclimatological reconstructions. *Journal of Biogeography* 31, 251–267.
- Solomon, S., Qin, D., Manning, M., Chen, Z., Marquis, M., Averyt, K. B., Tignor, M. & Miller, H. L. (eds). 2007: *Climate Change 2007: The Physical Science Basis. Contribution of Working Group I to the Fourth Assessment Report of the Intergovernmental Panel on Climate Change*. 996 pp. Cambridge University Press, Cambridge.
- Sonderogger, D. L. 2012: *SiZer: Significant zero crossings (R package version 0.1-5)*. Available at: <https://cran.r-project.org/web/packages/SiZer/>.
- Sonderogger, D. L., Wang, H., Clements, W. H. & Noon, B. R. 2009: Using SiZer to detect thresholds in ecological data. *Frontiers in Ecology and the Environment* 7, 190–195.
- Tallón, R., Costa, M., Schellekens, J., Taboada, T., Vives, J., Ferrer, C., Abel-Schaad, D., López-Sáez, J. A., Carrión, Y. & Martínez-Cortizas, A. 2014: Holocene environmental change in Eastern Spain reconstructed through the multiproxy study of a pedo-sedimentary sequence from Les Alcusses (Valencia, Spain). *Journal of Archaeological Science* 47, 22–38.
- Tarroso, P., Carrión, J. S., Dorado-Valiño, M., Queiroz, P., Santos, L., Valdeolmillos-Rodríguez, A., Alves, P. C., Brito, J. C. & Cheddadi, R. 2016: Spatial climate dynamics in the Iberian Peninsula since 15 000 BP. *Climate of the Past* 12, 1137–1149.
- Telford, R. J. & Birks, H. J. B. 2009: Evaluation of transfer functions in spatially structured environments. *Quaternary Science Reviews* 28, 1309–1316.
- Trouet, V., Esper, J., Graham, N. E., Baker, A., Scourse, J. D. & Frank, D. C. 2009: Persistent positive North Atlantic oscillation mode dominated the Medieval Climate Anomaly. *Science* 324, 78–79.
- Vasko, K., Toivonen, H. T. & Korhola, A. 2000: A Bayesian multinomial Gaussian response model for organism-based environmental reconstruction. *Journal of Paleolimnology* 24, 243–250.
- Visbeck, M. H., Hurrell, J. W., Polvani, L. & Cullen, H. M. 2001: The North Atlantic Oscillation: Past, present, and future. *Proceedings of the National Academy of Sciences of the United States of America* 98, 12876–12877.
- Vicente-Serrano, S. M., López-Moreno, J. I., Beguería, S., Lorenzo-Lacruz, J., Sánchez-Lorenzo, A., García-Ruiz, J. M., Azorín-Molina, C., Morán-Tejeda, E., Revuelto, J., Trigo, R., Coelho, F. & Espejo, F. 2014: Evidence of increasing drought severity caused by temperature rise in southern Europe. *Environmental Research Letters* 9, 044001. <https://doi.org/10.1088/1748-9326/9/4/044001>.

- Vidal-Macua, J. J., Ninyerola, M., Zabala, A., Domingo-Marimón, C. & Pons, X. 2017: Factors affecting forest dynamics in the Iberian Peninsula from 1987 to 2012. The role of topography and drought. *Forest Ecology and Management* 406, 290–306.
- Walker, M., Head, M. J., Berkelhammer, M., Björck, S., Cheng, H., Cwynar, L., Fisher, D., Gkinis, V., Long, A., Lowe, J., Newnham, R., Olander Rasmussen, S. & Weiss, H. 2018: Formal ratification of the subdivision of the Holocene Series/ Epoch (Quaternary System/ Period): two new Global Boundary Stratotype Sections and Points (GSSPs) and three new stages/ subseries. *Episodes* 41, 213–223.
- Weckström, J., Korhola, A., Erästö, P. & Holmström, L. 2006: Temperature patterns over the past eight centuries in northern Fennoscandia inferred from sedimentary diatoms. *Quaternary Research* 66, 78–86.
- Xoplaki, E., González-Rouco, F., Luterbacher, J. & Wanner, H. 2004: Wet season Mediterranean precipitation variability: influence of large scale dynamics and trends. *Climate Dynamics* 23, 63–78.

Supporting Information

Additional Supporting Information to this article is available at <http://www.boreas.dk>.

Fig. S1. Simplified pollen percentage diagrams for eight pollen records used in precipitation reconstructions. Only the 10 most common and important pollen taxa are shown. Black silhouettes indicate the percentage values and the unshaded silhouettes 10× exaggerations.

Fig. S2. Gaussian response curve for a taxon j determined by α_j (scaling factor), β_j (optimum precipitation) and γ_j (tolerance to precipitation).

Fig. S3. The colour-enhanced SiZer analysis (see the main text for further explanation) of the eight pollen records used in precipitation reconstructions based on WAPLS reconstructions. Upper panel for each record: WAPLS reconstruction for P_{ann} (mm a^{-1}). Lower panel for each record: the colour enhanced SiZer map which summarizes the statistical significance of the sign of the derivative of the smooths of the assumed true, unobserved P_{ann} , underlying the WAPLS reconstruction. Red colour indicates a decreasing trend (negative derivative) and blue colour indicates an increasing trend (positive derivative) as we read the data from past to present. Darker grey indicates a non-significant slope and lighter grey indicates that data are insufficient for the inference. The intensity of the colour indicates the magnitude of the increase or decrease. Vertical axis: logarithm of the level of smoothing h . With small values for $\log_{10}(h)$ we discover the small-scale features and the higher the value for $\log_{10}(h)$, the more smoothing is done and consequently the coarser the curve features discovered. From the SiZer map we can also infer where the maxima and

minima of P_{ann} occur as the colour changes from blue to red or from red to blue. See Table S3.

Fig. S4. P_{ann} reconstructions for eight pollen records using WAPLS and Bayesian models. The solid black line is the WAPLS reconstruction and the black dotted lines denote bootstrap estimated standard errors. The solid blue line is the posterior mean from the Bayesian model and the blue dotted lines show the point-wise 95% credible bands. The big black dot is the modern measured value for P_{ann} . The x -axis is time in years before present (age cal. a BP) and the y -axis is P_{ann} (mm a^{-1}).

Table S1. Information on the modern pollen samples. Modern annual precipitation (P_{ann}) values (mm) are obtained from the WorldClim database (Fick & Hijmans 2017) in a 30 s resolution (approximately 1 km^2). For each modern pollen sample name, longitude (W), latitude (N), P_{ann} (mm), altitude (m a.s.l.) and local vegetation are given.

Table S2. The prior distributions of the Bayesian model parameters. We denote by n and k the number of sites and the number of taxa in our modern calibration set. We denote by n_c the number of core slices studied in pollen record c , $c = 1, \dots, 8$. $P_{\text{ann}}(i)$ is the observed modern P_{ann} at site i and $P_{\text{ann}}(c)$ is the observed modern P_{ann} at the location of pollen record c . For definitions of the parameters, see Salonen *et al.* 2012.

Table S3. Main features of the SiZer maps for the eight pollen records used in precipitation reconstructions based on Fig. S3. Recall that the SiZer maps are shown only for the WAPLS reconstructions.

Table S4. Radiocarbon and depth data for eight fossil pollen records used for reconstructions. For each fossil pollen record the data is used to run the Bchron chronology model (see the outputs in Fig. 2). Bchron calibrates the radiocarbon dates and as an output we show the 95% credible intervals for the calibrated radiocarbon dates (age cal. a BP 95% CI). The top is not a radiocarbon date but it gives the extraction date in calendar years before present, the year 0 corresponding to AD 1950. References are the following: Monte Areo López-Merino *et al.* (2010), Alto de la Espina López-Merino (2009), Zalama Pérez-Díaz *et al.* (2016), Quintanar de la Sierra Peñalba *et al.* (1997), El Maíllo Morales-Molino *et al.* (2013), Navarrés-3 Carrión & van Geel (1999), San Rafael Pantaleón-Cano *et al.* (2003) and Padul-15-05 Ramos-Román *et al.* (2018a, b), Camuera *et al.* (2018).